Chapter 8

Conclusions and perspectives

8.1 Conclusions

This work proposes a study of a specific kind of actuators: the Flexible Fluidic Actuators. These are driven by fluid, i.e. gas or liquid, and present a flexible structure, i.e. an elastically deformable and/or inflatable structure. These actuators could be used to develop flexible instruments which could answer the need expressed by the medical community for such instruments. Hence this study is performed with a view to medical applications.

A review of the existing flexible fluidic actuators has been performed. It shows that there exist actuators able to stretch themselves, to shorten, to bend themselves or to develop a rotational motion and some of them present several DOFs. Two different methods to achieve bending have been identified. The first technique is based on "internal chambers differently pressurized" and the other one on "anisotropic rigidity". Besides, two methods to generate a rotational motion have also been identified. The actuators based on the first technique present a structure reinforced in places (with fibres or by increasing the material thickness) in such a way that when the actuators are pressurized, their structure involves a rotation. The second method to generate a rotational motion consists in an articulated structure in which one or several flexible fluidic actuators are inserted. When the actuators are pressurized, they actuate the structure which involves a rotation.
There exists a multitude of flexible fluidic devices and additional actuators can be obtained by combining different principles, in order to achieve more or less DOFs. Hence, this review can helps to develop medical flexible instruments based on flexible fluidic actuators. Indeed, according to the number and types of degrees of freedom required for the application, this review can help to choose a design. Besides, tools to be placed at the tips of the instruments could also be designed and based on flexible fluidic actuators.

According to the bulkiness that is allowed for the instrument in the targeted application, it will be necessary to assess the miniaturization potential of the actuators presented in the review. In this respect, actuators presenting a simple structure with a small number of parts will be better candidates to design miniature instruments. Since, miniaturizing the actuators also means miniaturizing their peripherics, some solutions have been presented in this respect.

Flexible fluidic actuators present interesting characteristics regarding an application inside the human body such as their compliance that allows them to handle delicate objects and to adapt themselves to their environment during contacts. Among the interesting features linked to the use of these actuators, one has caught our eye. Indeed, in [78], the "Flexible Microactuator" (FMA) is presented and it is suggested that the measurements of the fluid

pressure and of the volume of supplied fluid allow to determine and control the position of the actuator and the force it develops. This property has been called the "Pressure-Volume-Force-Position principle" or "PVFP principle" and it means being able to determine the displacement of a flexible fluidic actuator and the force it develops without using a displacement sensor or a force sensor [78].
This concept is particularly interesting for applications, such as medical ones, where the space is limited and where a miniaturization effort is required. This is for example the case in Teleoperated MIS where it is necessary to measure the force applied by the tools to the organs to ensure a force feedback of good quality. Obtaining this measurement is not straightforward. Indeed, if the force sensor is placed on the tool, outside the body of the patient, the measurement will be polluted by the friction of the trocar. To solve this problem, some researchers propose to place the sensor at the end of the tool inside the body but this raises the challenge to develop a small and sterilizable force sensor [63]. Using flexible fluidic actuators to actuate the surgical tools and exploiting the PVFP principle would allow to measure the force applied to the organs without the need for a force sensor.

A test bench has been developed to study and implement the PVFP principle and to characterize flexible fluidic actuators. It is basically a syringe-pump connected to the actuator to be studied. In practice, this syringe-pump is implemented with a linear motor that drives the piston of a cylinder whose output is connected to the actuator. This system uses a constant quantity of driving fluid and allows to pressurize the studied actuator. The test bench is equipped with different sensors that allow to measure the displacement of the cylinder piston, the pressure inside the actuator and the displacement(s) of its tip and weights are used to load the actuator. For the implementation of the PVFP principle, the volume of fluid supplied to the actuator is considered to be the volume swept by the cylinder piston and since this swept volume is proportional to the piston displacement, the latter will be the variable of interest instead of the swept volume.

To study and implement the PVFP principle, a flexible fluidic actuator called "Pneumatic Balloon Actuator" (PBA) has been used. This actuator, invented by [49], has been selected in the actuators review because it has a simple design, one DOF and because it is easily manufactured.

The implementation of the PVFP principle has consisted in characterizing the actuator by establishing experimental models of its behaviour. These models have then allowed to predict the displacements of the actuator tip and the weight attached to it, on the basis of the measurements of the piston displacement and of the pressure inside the actuator. This experimentally validates the PVFP principle in the case of the PBA. Concerning the quality of the predictions provided by the PVFP principle implemented on the flexible fluidic actuator, it to be evaluated with respect to a targeted application. Indeed, the predictions can be accurate enough for a given application but not for another one.
Hysteresis tests have been performed and it can be concluded that some of the PBA variables present some hysteresis; this hysteresis is not properly modeled by the experimental models. However, before modeling the hysteresis, it has to be assessed whether this hysteresis is problematic or not with respect to the targeted application. Indeed, for a given application, the hysteresis may be small enough to be negligible; in this case, there is no need to model the hysteresis. On the other hand, for another application, the same hysteresis may be too large to be ignored; in this case, it has to be modeled properly and this requires the elaboration of new experimental models of the PBA.

A numerical model of the PBA has been established by modeling the physics that seem to rule it. This model has been built in collaboration with the PMA department of the

KUL. The actuator is modeled as the combination of a membrane and a beam. A PBA modeled with the numerical model will be less stiff than its real counterpart and some of the assumptions on which the model rests are not verified in reality; this leads to large differences between the predictions provided by the model and the measurements performed on the prototypes (the PBA described in [49] and the PBA developed for the test bench). However, the numerical model is able to predict the bidirectional behaviour of a PBA and allows to better understand the physics underlying. The bidirectional behaviour is due to the pressure applied to the beam and to the force applied by the pressurized membrane to the beam. If the force applied by the membrane is predominant, the PBA free end moves upwards while if the pressure is predominant, it moves downwards.
It has to be mentioned that the numerical model seems to predict that all PBAs show this bidirectional behaviour while in practice, this behaviour has been reported for PBAs completely made of the same material and it is not established whether this behaviour happens for PBAs whose layers are made of different materials.
However, at this stage, it is not possible to conclude whether the numerical model could be used to predict the qualitative effects, on the tip displacements, of the change of a PBA parameter.

A miniaturization work has been performed on a particular kind of flexible fluidic actuator: the Pleated Pneumatic Artificial Muscle (PPAM). This actuator has been developed at the Department of Mechanical Engineering of the Vrije Universiteit Brussel (VUB).
According to theoretical models, miniaturized PPAMs, whose dimensions are small enough to be inserted into MIS medical instruments, could be able to develop the forces required to allow the instruments to perform most surgical actions. Therefore, the PPAMs have been studied in order to assess their miniaturization potential. This miniaturization work has been performed by Nhat-Quang CAO as a Master's thesis, in collaboration with the VUB.
The miniaturization work has been performed on the third generation PPAMs developed at the VUB and for this first attempt, the target was to develop a miniaturized muscle able to develop a force of about 100 N and having a diameter at rest of about 1 cm. No specific objective was set concerning the stroke of the muscle.
The achieved miniaturized muscles have a design similar to that of the third generation PPAMs developed at the VUB and present a total length of about 90 mm and an outer diameter at rest of about 15 mm. They are twice as small as the third generation PPAM of the VUB. Two miniaturized muscles have been characterized experimentally. For pressure levels ranging between 0.3 bar and 0.6 bar, the maximum contractions of the first muscle range between 5.7 % and 8 %. The second muscle presents better characteristics than the first one and this is due to the better regularity of its folds. Indeed, for given pressure and contraction, the second muscle develops a larger force than the first one. Besides, it better goes back to its initial cylindrical shape when it is depressurized and for the same pressure levels as the first muscle, its maximum contractions seem to be larger.
The first miniaturized PPAM has also been pressurized at $p = 1$ bar and it was able to develop a pulling force $F = 100$ N while producing a contraction $\epsilon = 4$ %. Hence, it can be concluded that the miniaturization objectives have been reached concerning the developed force while the diameter should be further reduced.

For the PBAs as well as for the PPAMs, it is not possible to impose the actuator displacement(s) and the force it develops at the same time. In practical applications, a choice will have to be made between imposing the force and imposing the displacements, according to the task to be performed.

8.2 Perspectives

The PVFP principle has been experimentally validated with the PBA, i.e. an actuator presenting only one DOF. With such an actuator, the applied force can be predicted at only one precise point and along only one precise direction. However, the principle can probably be applied to more complex structures presenting several chambers to be pressurized.

The PVFP principle could be implemented in a control loop in order to control the displacement of a flexible fluidic actuator tip or the force it develops, without using a displacement or a force sensor.

To implement this principle in a real medical application, it needs to be robust to the external perturbations such as a change in the ambient atmospheric pressure or temperature. Concerning the PBA, the PVFP principle seems applicable to this actuator with an incompressible or a compressible actuation fluid. Besides, if the PVFP principle is implemented on the PBA with an incompressible fluid and if a gauge pressure is used to measure the actuator pressure, it seems that the predictions provided by the PVFP principle implemented on the actuator will not be influenced by the changes of the atmospheric pressure and of the temperature.
For medical applications, a physiological saline solution can be used as incompressible fluid all the more that gas leakages are forbidden in some applications.

Replacing gas by liquid brings also the advantage that the system gets rid of the compressibility of the actuation fluid and this may decrease the establishing time of the pressure in the fluidic circuit. Indeed, during the experiments presented in this work, it has been noticed that the gas pressure takes several minutes to stabilize after a piston displacement.The fact that the pressure needs a long time to stabilize can be accredited to the gas compressibility, to the elasticity of the pneumatic tubes and to the elasticity of the flexible fluidic actuator. Studying the quantitative effect of each of these three causes would help to determine which action to take in order to reduce the establishment time of the pressure in the fluidic circuit and to increase the bandwidth of the system. However, before performing this study, it would be interesting to study the sensibility of the actuator displacements with regard to the pressure establishment. Indeed, it has a small effect on the actuator displacements, it may be superfluous to make a thorough study of the pressure dynamics.

Replacing gas by liquid implies larger pressure losses whose effect has to be studied. Besides, a flexible fluidic actuator filled with liquid will be heavier and as a consequence it will develop smaller displacements, for a given pressure level, than the same actuator filled with gas. Hence, the actuator will probably present a pressure threshold because a minimum pressure level will be required to compensate the weight of the liquid. An actuator filled with liquid will also be less compliant. All these aspects could be studied in future works.

Concerning the numerical model of the PBA, it could be modified in order to predict the displacements of the actuator tip rather than the displacements of the cavity tip. This would allow a better comparison between the predictions of the numerical model and the measurements performed on Konishi's PBA and the test bench PBA.
More experimental validations should be made with prototypes whose parameters are perfectly known in order to determine whether the numerical model could be used to predict the qualitative effects, on the tip displacements, of the change of a PBA parameter.

Concerning the miniaturized PPAMs, other tests on other miniaturized muscles will be necessary to verify the repeatability of the results, to study more thoroughly the hysteresis of the muscle, to assess its life duration and to determine the maximum force and contraction the muscle can produce and the maximum pressure it can bear. Besides, dynamical tests could be performed to determine the dynamical characteristics of the miniaturized muscles. Regarding a further miniaturization of the muscles, propositions have been made and could be tested in future works.

Appendix A

Test bench

A.1 Design of the syringe-pump test bench: comparison of the different considered solutions

A syringe-pump design is chosen for the test bench. The flexible fluidic actuator will be connected to the output of the syringe-pump and this will create a fluidic circuit composed of the chamber of the syringe-pump, the connection tubes and the flexible fluidic actuator. When the piston of the syringe-pump will be actuated, the pressure in the fluidic circuit will increase or decrease according to the actuation direction and the actuator will be actuated.
In practice, a cylinder will be used as the syringe (see no. 5 in Fig. A.1). Besides, although a syringe-pump design can be used with gas or liquid, air will be used as fluid. Indeed, this will ease the use of the test bench because air is a readily available source, it can be freely evacuated in the ambient air [70] and possible leakages will not risk damaging the test bench (e.g. the electrical connections).
The volume of fluid supplied to the actuator is considered to be the volume swept by the piston of the syringe-pump. Hence, this volume is proportional to the displacement of the cylinder piston and in practice, the piston displacement is the variable that will be used instead of the swept volume.
The principle of the test bench is presented in Fig. A.1 and consists in the actuation of the cylinder piston (no. 4 in Fig. A.1) by an actuator (no. 1 in Fig. A.1). This actuator will be equipped with a position sensor to measure the displacement of the cylinder piston.

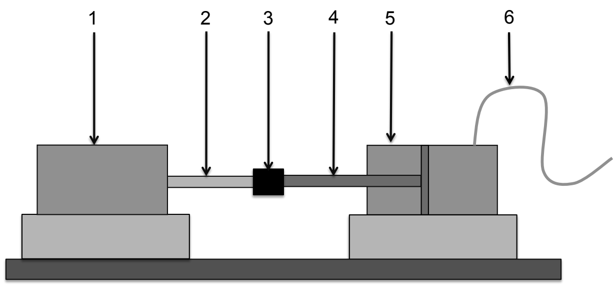

Figure A.1: Scheme of the syringe-pump test bench: 1) actuator + position sensor 2) shaft of the actuator 3) linking part 4) pneumatic cylinder piston 5) pneumatic cylinder 6) pneumatic tube (it connects the flexible fluidic actuator to the output of the cylinder)

Four possible solutions have been considered for the implementation of the test bench; they are presented here and compared regarding the implementation difficulty.

A.1.1 Basic solution: nothing is integrated, all the components are chosen separately and assembled together

Description

Fig. A.2 presents the first solution. A DC or stepper motor (no. 2 in Fig. A.2), equipped with an encoder, is coupled to a ball screw (no. 4 in Fig. A.2), supporting a ball nut (no. 5 in Fig. A.2). This nut is linked to the slider (no. 10 in Fig. A.2) of a linear guide (no. 11 in Fig. A.2) and the slider is linked to the piston of the cylinder (no. 7 in Fig. A.2). When the motor rotates, it drives the ball screw. The nut moves along the ball screw, the slider is driven along the linear guide and the cylinder piston is displaced. The encoder measures the rotation of the motor and allows to compute the displacement of the cylinder piston.

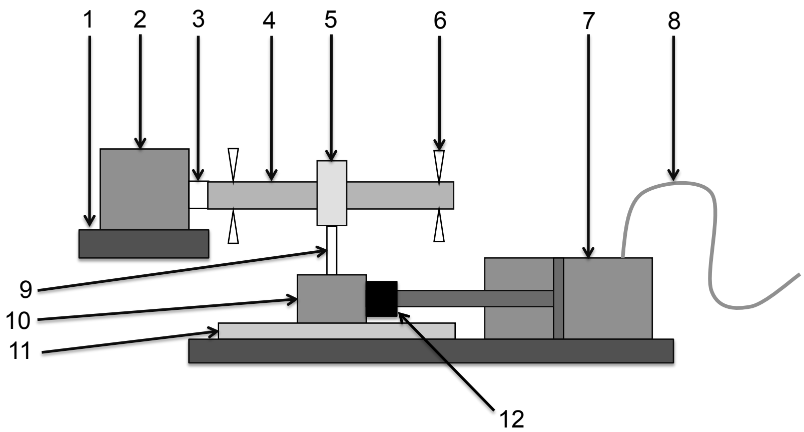

Figure A.2: First solution to implement the syringe-pump test bench: nothing is integrated, all the components are chosen separately and assembled together. 1) mounting parts of the motor 2) DC or stepper motor + encoder 3) coupling parts 4) ball screw 5) ball nut 6) support bearings of the ball screw 7) pneumatic cylinder 8) pneumatic tubes 9) linking part between the ball nut and the slider 10) slider 11) linear guide 12) linking part between the slider and the cylinder piston

Discussion

With this solution, nothing is integrated and all the parts are chosen separately. To assemble them, extra parts need to be ordered or designed and manufactured. Indeed, :

- To be fixed, the motor needs mounting parts (no. 1 in Fig. A.2). These parts need to be manufactured.
- To assemble the motor and the ball screw, coupling parts are necessary (no. 3 in Fig. A.2). These can be chosen off the shelf.
- The ball screw needs support bearings (no. 6 in Fig. A.2). These can be chosen off the shelf.

- The part linking the ball nut and the slider needs to be manufactured (no. 9 in Fig. A.2). This part will be subjected to shear and needs to be correctly designed to bear these stresses.
- The part linking the slider and the cylinder piston needs to be manufactured (no. 12 in Fig. A.2).

Besides,

- The motor and the ball screw need to be correctly aligned as well as the ball screw and the linear guide and the linear guide and the cylinder piston, to avoid out-of-axis efforts. Indeed, the motor, the linear guide and the cylinder piston can bear limited out-of-axis efforts and moreover, these efforts could cause friction and loss of positioning accuracy.
- The ball screw has a limited maximum rotational speed.
- The rotational motor can bear a limited axial load and a limited radial load.
- The slider sliding in the linear guide can bear limited efforts (forces and torques).
- The backlash resulting from the assembly of all the parts of the system needs to stay acceptable with regard to the wanted positioning accuracy.

In conclusion, the implementation of this first solution is quite difficult because of all the components limitations that have to be taken into account and because of the large number of parts that need to be selected or designed and manufactured.

A.1.2 The motor and the ball screw are integrated

Description

There exist motors already combined with a ball screw supporting a nut. For example, Maxon Motor [16] proposes "Modular spindle drives" (see Fig. A.3)

Figure A.3: "Modular spindle drive" proposed by Maxon Motors. Figure from [7].

The second solution is thus the same as the first solution apart from that the motor and the ball screw are integrated.

Discussion

This second solution brings the following advantages in comparison with the first solution:

- The integrated module "motor + ball screw" is designed to support higher axial loads than classical motors.
- The coupling between the motor and the ball screw is already done. As a consequence, no coupling part needs to be chosen and ordered.
- The alignment between the motor and the ball screw is already done.

A.1.3 The ball screw and the linear guide are integrated

Description

There exist devices including the ball screw and the linear guide into one linear module. For example, the THK company [21] proposes "LM guide actuators Model KR". As can be seen in Fig. A.4, these devices present:

- mounting parts for the motor
- a ball screw
- a ball train that slides in a rail
- support bearings for the ball screw

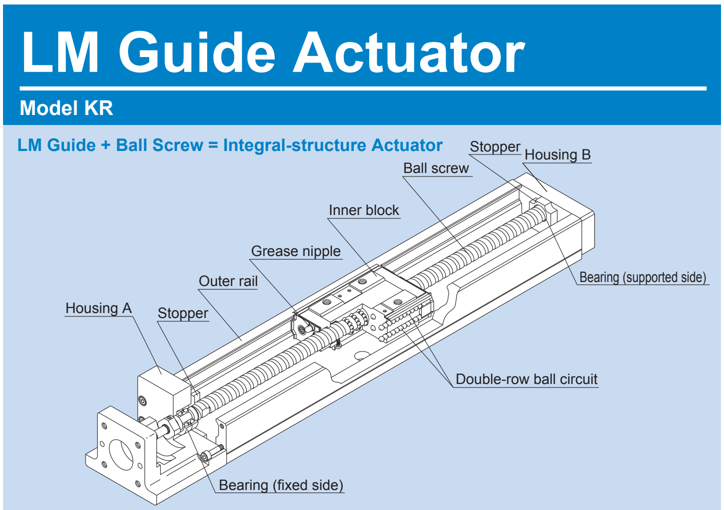

Figure A.4: "LM guide actuator Model KR" proposed by THK. Figure from [15].

Fig. A.5 presents a scheme of the implementation of the test bench based on such a linear module. As can be seen, in addition to selecting a linear module (parts no. 1, 4, 6, 7 and 8 in Fig. A.5 are integrated into the linear module), implementing this solution requires to select coupling parts (no. 3 in Fig. A.5) and a motor equipped with an encoder (no. 2 in Fig. A.5), to design and manufacture a linking part (no. 5 in Fig. A.5) for the ball train (no. 7 in Fig. A.5) and the cylinder piston (no. 9 in Fig. A.5) and to align the linear module and the cylinder piston.

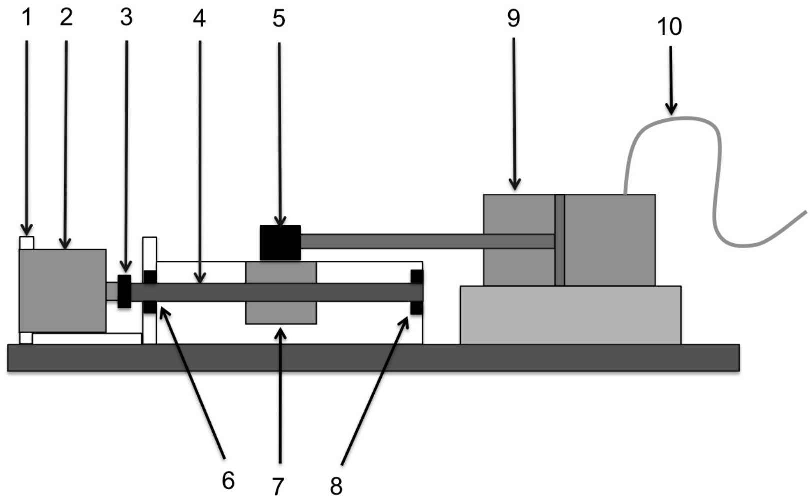

Figure A.5: Third solution to implement the syringe-pump test bench: 1) mounting parts of the motor 2) DC or stepper motor + encoder 3) coupling parts 4) ball screw 5) linking part between the ball train and the cylinder piston 6) support bearings 7) ball train 8) support bearings 9) pneumatic cylinder 10) pneumatic tubes. Parts no. 1, 4, 6, 7 and 8 are integrated into a linear module.

Discussion

With such an integrated unit, the third solution presents the following advantages in comparison with the first solution:

- The support bearings of the ball screw are already provided.
- Mounting parts are already provided for the motor.
- A linking part between the ball screw and the linear guide is no longer needed since the ball train slides in the guide.
- The alignment between the ball screw and the linear guide is already done.
- The alignment between the motor and the ball screw is easily performed since the motor only needs to be placed in the mounting parts.
- The linear module limits the risk of backlash in comparison with the first design solution.

A.1.4 Linear actuator

Description

A fourth solution consists in using a linear actuator to actuate the cylinder piston. A linear actuator can be a linear motor, such as those proposed by the LinMot company [14] (see Fig. A.6), or an integrated system "motor - screw - sliding shaft" such as those provided by the Danaher Motion company[1] [10] (see Fig. A.7).

[1]Danaher Motion describes its electric linear actuators as follows: "The design of an electric linear actuator is quite basic. An electric motor - through either a timing belt, a gear drive or via in-line direct coupling - rotates a ball screw or acme screw, which translates the torque into axial force through the extension tube" [5].

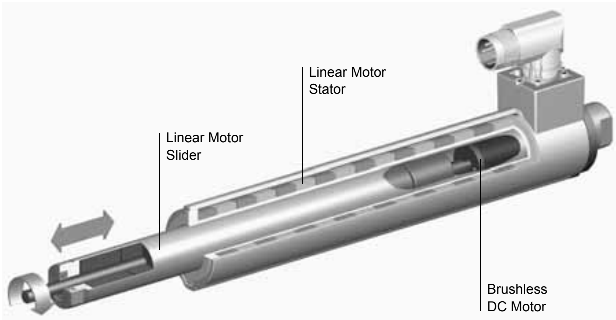

Figure A.6: Linear motor proposed by LinMot. Figure from [1].

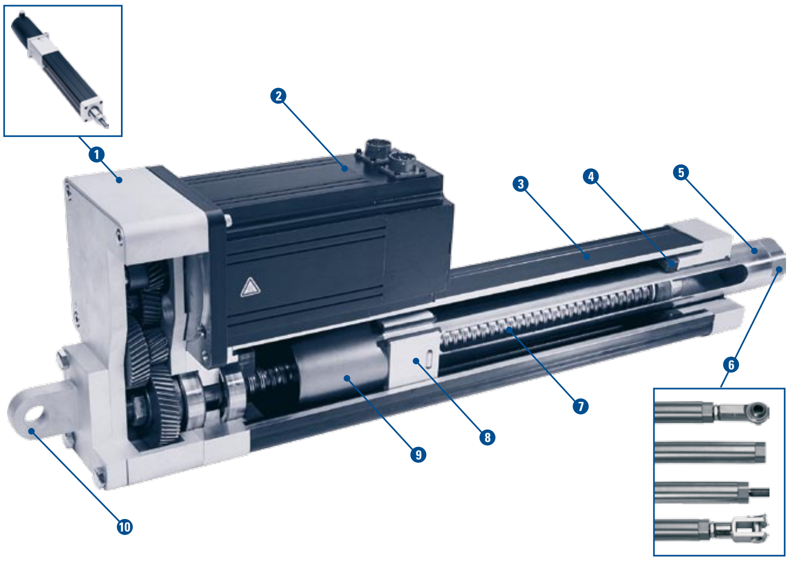

1. **Parallel mounted motor with belt or helical gear or in-line motor with direct drive or planetary gear.**
2. **Permanent magnet DC motor, Brushless AC servo motor or three phase AC motor with or without integrated brake.**
3. **Stiff and strong extruded aluminium cover tube with integrated magnetic sensor grooves.**
4. **High quality extension tube seals protect the actuator from penetration of dust, dirt and liquids.**
5. **Robust stainless steel extension tube.**
6. **Choose between extension tube with inside or outside thread, clevis or spherical joint ends.**
7. **Acme or ball screw transmission.**
8. **Internally guided extension tube with anti-rotation mechanism which also acts as a screw support.**
9. **Shock load resistant acme nut or high-precision safety ball nut.**
10. **Mounting kits such as clevis, trunnion, mounting feet and front /rear flange available.**

Figure A.7: "Electric linear actuator" proposed by Danaher Motion. Figure from [5].

As shown in Fig. A.8, to set up this fourth solution, the linear actuator equipped with a position sensor (no. 1 in Fig. A.8) only needs to be aligned with the cylinder piston (no. 4 in Fig. A.8) and a part (no. 3 in Fig. A.8) linking the cylinder piston and the sliding shaft of the linear actuator (no. 2 in Fig. A.8) needs to be manufactured.

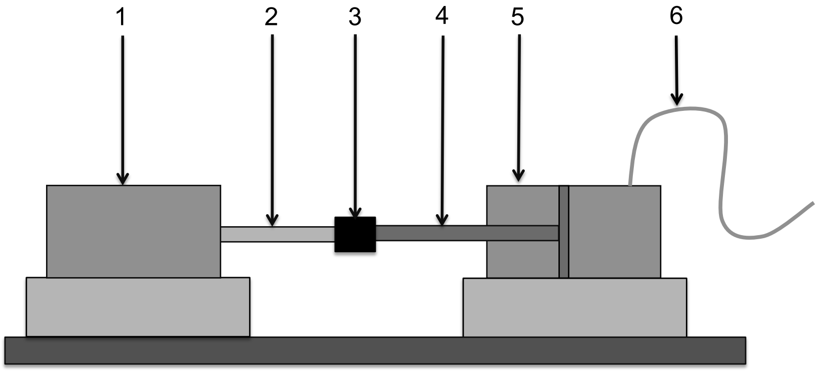

Figure A.8: Fourth solution to implement the syringe-pump test bench: 1) linear actuator + position sensor 2) sliding shaft of the linear actuator 3) part linking the shaft of the linear actuator and the piston of the pneumatic cylinder 4) piston of the pneumatic cylinder 5) pneumatic cylinder 6) pneumatic tubes

Discussion

Since they are designed to produce linear motions, linear actuators can presumably bear higher axial loads than the motors of the first and third solutions. Moreover, among the linear actuators, the linear motors have presumably a better positioning accuracy because they are composed only of a magnetic slider sliding in a stator while the other types of linear actuators are made of several parts assembled together.
Among the four considered solutions, the fourth one is the easiest to implement.

A.1.5 Conclusions

To ease the setting up of the test bench, the fourth solution has been chosen because most of its parts are already integrated. Besides, a linear motor has been preferred to another type of linear actuator in order to have a better positioning accuracy.

A.2 Linmot linear motor

A.2.1 List of all the ordered Linmot components (motor + accessories)

Technical components
AL-Profiles
Linear motors
Pneumatic units
Conveyors
Special Bearings
Axes
Machine Design

PROFILEX s.a.

4A, Z.I. In den Allern
L-9911 TROISVIERGES

Tél.: 00352/99 89 06
Fax : 00352/26 95 73-73

profilex@pt.lu
www.profilex-systems.com

UNIVERSITE LIBRE DE BRUXELLES
Mad.De Greef
Av. F.D. Roosevelt, 50 CP 165/55
B-1050 BRUSSEL 0

OFFRE 280201
Personne de contact : Manfred Backes

Fax : +32-2-650-47-24

Date	Page	Client	N° TVA	Référence : Offre de prix actualisée
20/06/08	1 de 1	ULB1	BE0407.626.464	

Pos	N° article	Désignation	Dimens.	Unité	Quant.	Prix unit.	Rab %	Montant
		Nous vous remercions de votre demande de prix aimable et avons le plaisir de vous offrir:						
1	L0150-1943	POWER SUPPLY 72V/600W/ S01-72/600		pc	1	757,940	15,0	644,25
2	L0150-1381	SLIDER PL01-28x410/330 F.LIN.MOTOR 4		pc	1	817,500	15,0	694,88
3	L0150-1219	LINEAR MOTOR STATOR PS01-48x240-C		pc	1	637,920	15,0	542,23
4	L0150-1975	MOUNTING FLANGE PF01-48x240		pc	1	74,200	15,0	63,07
5	L0150-5051	Fan cooling for H01-37/48 & PF01-48		pc	1	28,460	15,0	24,19
6	L0150-1801	CABLE K15-W/C-04M EXTENSION/IP67-I		pc	1	165,620	15,0	140,78
7	L0150-1685	CONTROLLER B 1100 VF 48-72V/8A		pc.	1	349,730	15,0	297,27
8	L0150-3087	FIXED END WASHER SET FOR 28 MM SI		pc	1	5,280	15,0	4,49
9	L0150-3094	PLL01-28 FLOATING BEARING F.28 MM		pc	1	35,970	15,0	30,57
10	L0150-1840	MAGNET SENSOR 1µm, A/B(for 1 mm pit		m	1	394,520	15,0	335,34
11	L0150-1963	MAGNETIC STRIP MB01-1000 , 1MM PIT	0,2700	m	1	346,000	15,0	79,41
12	TRANS	PORT		pc	1	17,720		17,72
13	ASSU	ASSURANCE TRANSPORT		pc	1	10,440		10,44
		Délai : 7-10 jours						
		Payement: endans 30 jours date de facture net.						
		Validité : 60 jours						

TVA		Base	Montant
G	0 %	2.884,64	0,00

Total remise 504,08 €

Total hors TVA	2.884,64
Total TVA	0,00
TOTAL EUR	**2.884,64**

Toute livraison est effectuée exclusivement à base de nos conditions de vente avec clause de propriété imprimées au verso, sauf contraire écrit.
Al onze leveringen geschieden exclusief op basis van onze algemene verkoopsvorwaarden op verso, inklusief eigendoomsvoorbehoudt, voorzover niet schiftlijk anders overeengekomen.
Alle Lieferungen werden ausschliesslich nach unseren rückseitig gedruckten Verkaufsbedingungen, inklusiv Eigentumsvorbehalt, ausgeführt, sofern nicht anders schriftlich vereinbart.

Signature client, date et cachet:
Handtekening klant, datum en stempel:
Kundenunterschrift, Datum und Stempel:

Figure A.9: Order of the linear motor and its accessories

A.2.2 The S and SS strokes of the Linmot motors

The Linmot linear motors are characterized by two kinds of strokes (see Fig. A.10):

- a maximum stroke S: it is the maximum displacement that the slider can reach.
- a shortened stroke SS: it is the part of the stroke S on which the motor can develop its maximum peak force.

The evolution of the peak force along the stroke has a trapezoidal shape and the centre of the stroke range is called the "zero position (ZP)". The available peak force is thus dependent on the slider position but it is also dependent on the maximum current from the servo controller.

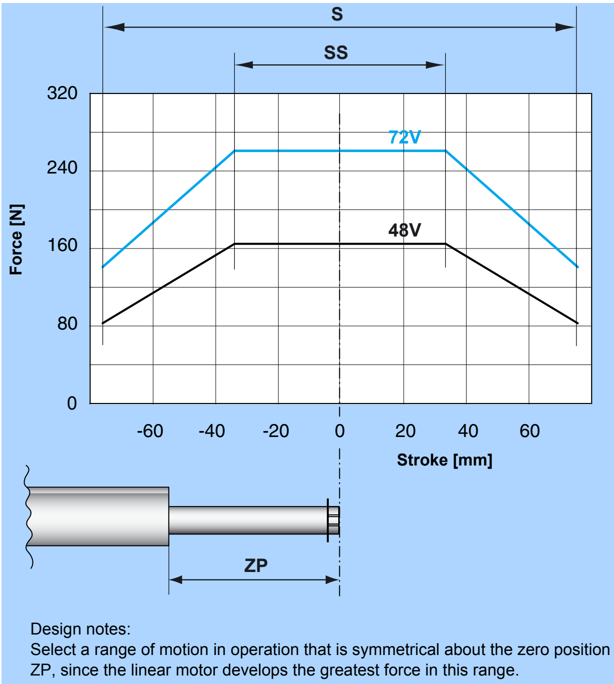

Figure A.10: Linmot linear motors: description of the maximum stroke S, of the shortened stroke SS and of the zero position ZP. The evolution of the peak force along the stroke has a trapezoidal shape. Both curves correspond to different servo controllers. Figure from [1].

A.2.3 Characteristics of the Linmot motor chosen for the test bench

The characteristics of the chosen Linmot motor are presented in Fig. A.11.

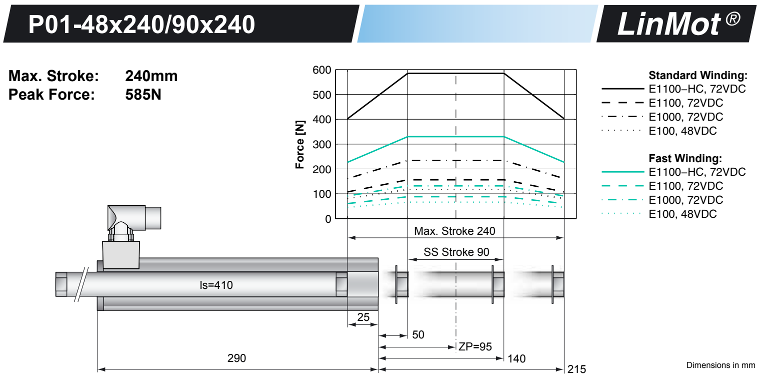

Motor Specification

	P01-	Standard Winding 48x240/90x240-C	Fast Winding 48x240F/90x240-C
Stroke Max.	mm (in)	240 (9.45)	240 (9.45)
Stroke SS	mm (in)	90 (3.54)	90 (3.54)
Peak Force E100/1000	N (lbf)	117/234 (26.3/52.6)	66/132 (14.8/29.7)
Peak Force E1100/-HC	N (lbf)	156/585 (35.1/131.5)	88/330 (19.8/74.2)
Cont. Force	N (lbf)	145 (32.6)	145 (32.6)
Cont. Force Fan cooling	N (lbf)	257 (57.8)	257 (57.8)
Border Force	%	69	69
Force Constant	N/A (lbf/A)	39.0 (8.77)	22.0 (4.95)
Max. Current @ 72VDC	A	15.0	15.0
Max. Current @ 48VDC	A	11.5	15.0
Max. Velocity @ 72VDC	m/s (in/s)	1.7 (67)	3.0 (119)
Max. Velocity @ 48VDC	m/s (in/s)	1.1 (45)	2.0 (79)
Phase Resist. 25/80 °C	Ohm	3.1/3.7	1.0/1.2
Phase Inductance	mH	3.1	1.0
Thermal Resistance	°K/W	1.1	1.1
Thermal Time Const.	sec	3000	3000
Stator Diameter	mm (in)	48 (1.89)	48 (1.89)
Stator Length	mm (in)	290 (11.40)	290 (11.40)
Stator Mass	g (lb)	1930 (4.25)	1930 (4.25)
Slider Diameter	mm (in)	28 (1.10)	28 (1.10)
Slider Length	mm (in)	410 (16.14)	410 (16.14)
Slider Mass	g (lb)	1740 (3.84)	1740 (3.84)
Position Repeatability	mm (in)	±0.05 (±0.0020)	±0.05 (±0.0020)
Linearity	%	±0.2	±0.2
Position Rep. with ES	mm (in)	±0.01 (±0.0004)	±0.01 (±0.0004)
Linearity with ES	mm (in)	±0.01 (±0.0004)	±0.01 (±0.0004)

Position-Time Diagram

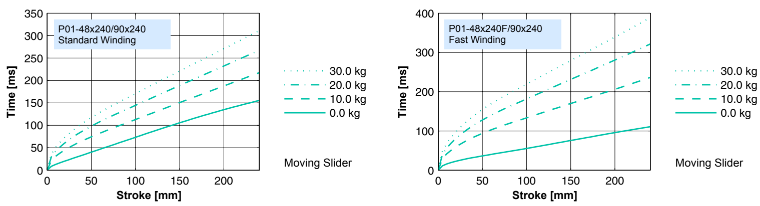

244 www.LinMot.com

Figure A.11: Characteristics of the PO1-48X240/90X240 Linmot linear motor. Figure from [1].

The motor is installed in a flange (see Fig. A.12) and is cooled by a fan (see Fig. A.13).

Figure A.12: Linear motor equipped with a flange (black part). Figure from [1].

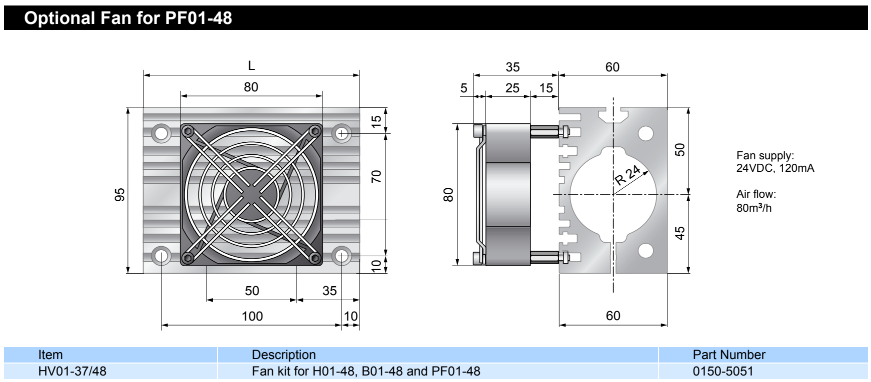

Figure A.13: Fan of the Linmot linear motor. Figure from [1].

Besides, it is equipped with an external position sensor (see Fig. A.14 and A.15).

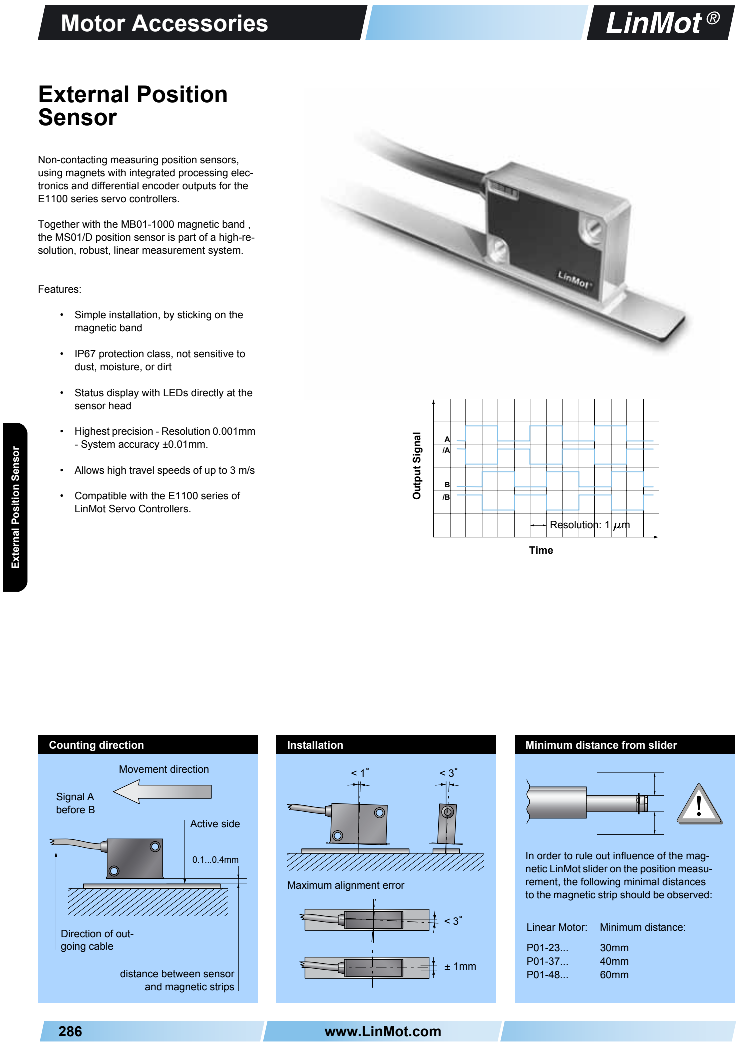

Figure A.14: External position sensor and magnetic strip. Figure from [1].

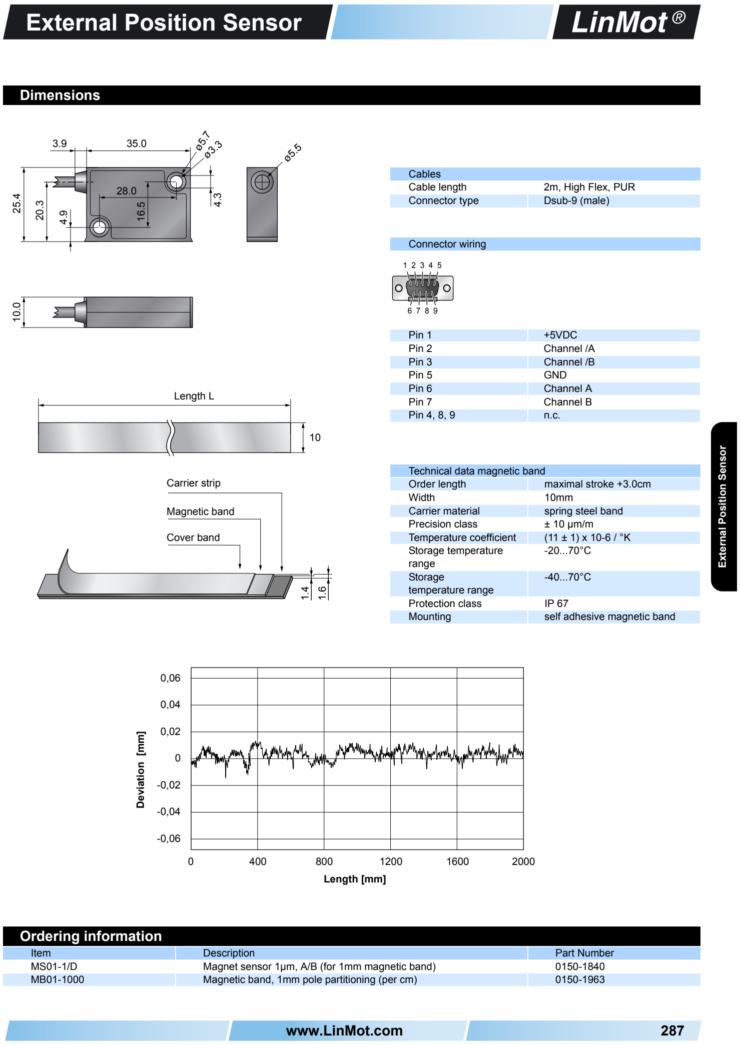

External Position Sensor — LinMot®

Dimensions

Cables	
Cable length	2m, High Flex, PUR
Connector type	Dsub-9 (male)

Connector wiring	
Pin 1	+5VDC
Pin 2	Channel /A
Pin 3	Channel /B
Pin 5	GND
Pin 6	Channel A
Pin 7	Channel B
Pin 4, 8, 9	n.c.

Technical data magnetic band	
Order length	maximal stroke +3.0cm
Width	10mm
Carrier material	spring steel band
Precision class	± 10 µm/m
Temperature coefficient	(11 ± 1) x 10-6 / °K
Storage temperature range	-20...70°C
Storage temperature range	-40...70°C
Protection class	IP 67
Mounting	self adhesive magnetic band

Ordering information

Item	Description	Part Number
MS01-1/D	Magnet sensor 1µm, A/B (for 1mm magnetic band)	0150-1840
MB01-1000	Magnetic band, 1mm pole partitioning (per cm)	0150-1963

www.LinMot.com 287

Figure A.15: External position sensor and magnetic strip. Figure from [1].

A B1100-VF controller (see Fig. A.16, A.17 and A.18) has been chosen for the motor.

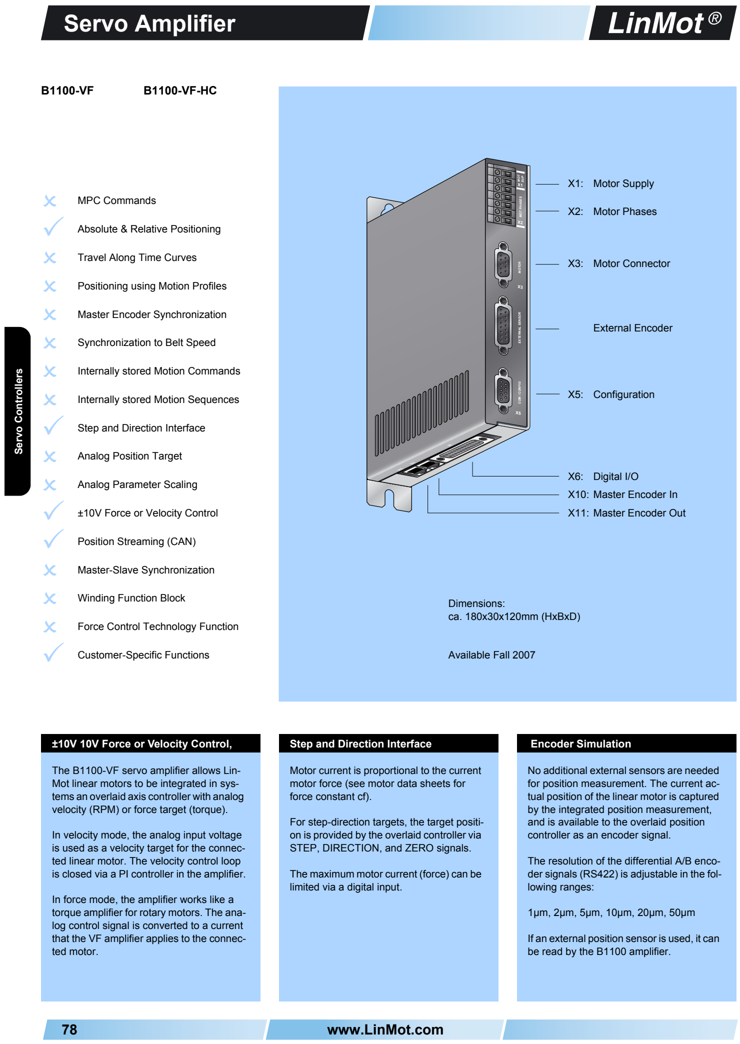

Servo Amplifier LinMot®

B1100-VF B1100-VF-HC

Servo Controllers

- ✗ MPC Commands
- ✓ Absolute & Relative Positioning
- ✗ Travel Along Time Curves
- ✗ Positioning using Motion Profiles
- ✗ Master Encoder Synchronization
- ✗ Synchronization to Belt Speed
- ✗ Internally stored Motion Commands
- ✗ Internally stored Motion Sequences
- ✓ Step and Direction Interface
- ✗ Analog Position Target
- ✗ Analog Parameter Scaling
- ✓ ±10V Force or Velocity Control
- ✓ Position Streaming (CAN)
- ✗ Master-Slave Synchronization
- ✗ Winding Function Block
- ✗ Force Control Technology Function
- ✓ Customer-Specific Functions

Dimensions:
ca. 180x30x120mm (HxBxD)

Available Fall 2007

±10V 10V Force or Velocity Control,

The B1100-VF servo amplifier allows LinMot linear motors to be integrated in systems an overlaid axis controller with analog velocity (RPM) or force target (torque).

In velocity mode, the analog input voltage is used as a velocity target for the connected linear motor. The velocity control loop is closed via a PI controller in the amplifier.

In force mode, the amplifier works like a torque amplifier for rotary motors. The analog control signal is converted to a current that the VF amplifier applies to the connected motor.

Step and Direction Interface

Motor current is proportional to the current motor force (see motor data sheets for force constant cf).

For step-direction targets, the target position is provided by the overlaid controller via STEP, DIRECTION, and ZERO signals.

The maximum motor current (force) can be limited via a digital input.

Encoder Simulation

No additional external sensors are needed for position measurement. The current actual position of the linear motor is captured by the integrated position measurement, and is available to the overlaid position controller as an encoder signal.

The resolution of the differential A/B encoder signals (RS422) is adjustable in the following ranges:

1µm, 2µm, 5µm, 10µm, 20µm, 50µm

If an external position sensor is used, it can be read by the B1100 amplifier.

78 www.LinMot.com

Figure A.16: Datasheet of the B1100-VF controller. Figure from [1].

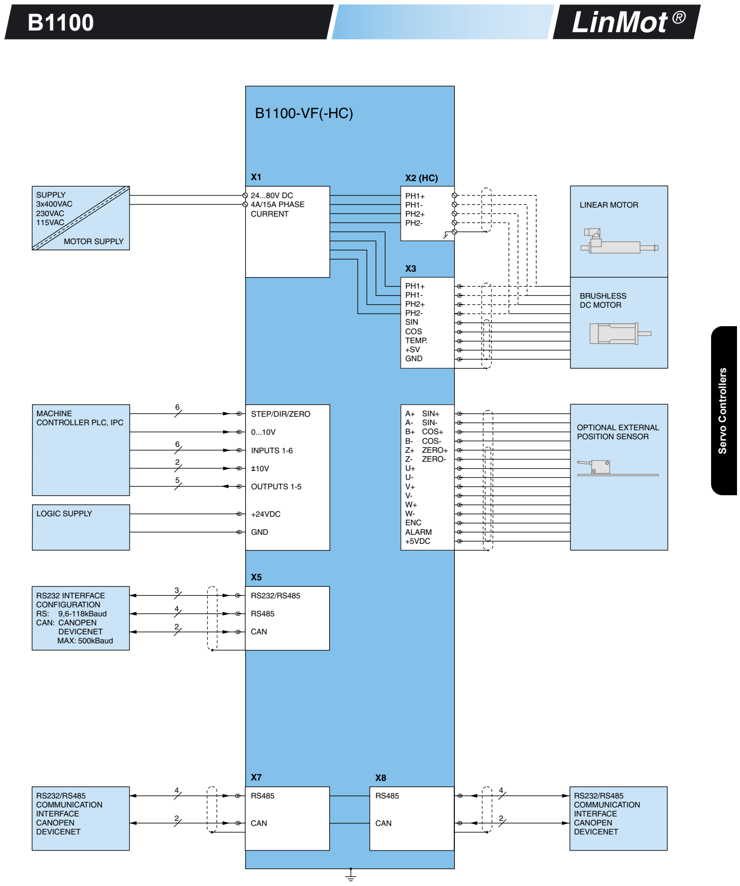

Item	Description	Part Number
B1100-VF	VF-Controller (72V/4A)	0150-1685
B1100-VF-HC	VF-Controller (72V/15A)	0150-1686

www.LinMot.com 79

Figure A.17: Datasheet of the B1100-VF controller. Figure from [1].

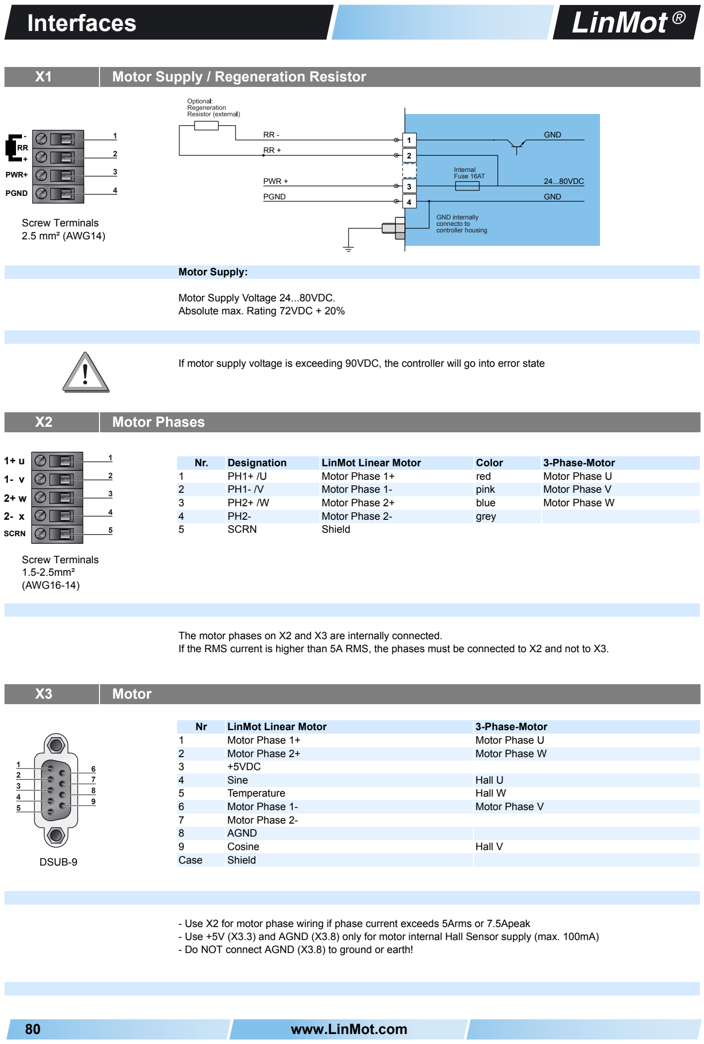

Interfaces

LinMot®

X1 Motor Supply / Regeneration Resistor

Screw Terminals
2.5 mm² (AWG14)

Motor Supply:

Motor Supply Voltage 24...80VDC.
Absolute max. Rating 72VDC + 20%

If motor supply voltage is exceeding 90VDC, the controller will go into error state

E1100

X2 Motor Phases

Nr.	Designation	LinMot Linear Motor	Color	3-Phase-Motor
1	PH1+ /U	Motor Phase 1+	red	Motor Phase U
2	PH1- /V	Motor Phase 1-	pink	Motor Phase V
3	PH2+ /W	Motor Phase 2+	blue	Motor Phase W
4	PH2-	Motor Phase 2-	grey	
5	SCRN	Shield		

Screw Terminals
1.5-2.5mm²
(AWG16-14)

The motor phases on X2 and X3 are internally connected.
If the RMS current is higher than 5A RMS, the phases must be connected to X2 and not to X3.

X3 Motor

Nr	LinMot Linear Motor	3-Phase-Motor
1	Motor Phase 1+	Motor Phase U
2	Motor Phase 2+	Motor Phase W
3	+5VDC	
4	Sine	Hall U
5	Temperature	Hall W
6	Motor Phase 1-	Motor Phase V
7	Motor Phase 2-	
8	AGND	
9	Cosine	Hall V
Case	Shield	

DSUB-9

- Use X2 for motor phase wiring if phase current exceeds 5Arms or 7.5Apeak
- Use +5V (X3.3) and AGND (X3.8) only for motor internal Hall Sensor supply (max. 100mA)
- Do NOT connect AGND (X3.8) to ground or earth!

80 www.LinMot.com

Figure A.18: Datasheet of the B1100-VF controller. Figure from [1].

Fig. A.19 and A.20 present the datasheets of the 72 V/600 W power supply of the linear motor.

Servo Controllers **LinMot®**

Switched-Mode Power Supplies

Servo Controller Accessories

Switched-Mode Power Supplies								
Output voltage		**24V**		**48V**			**72V**	
Input voltage		150W	300 W	150 W	300 W	600 W	300W	600W
Input Specification								
Input voltage range	[VAC]	93...123 / 187...264						
Input frequency	[Hz]	47...63						
Input current at full load (230V)	[A]	1.7	3.3	1.7	3.3	6.4	3.3	6.4
Input current at full load (115V)	[A]	3	5.4	3	5.4	10.5	5.4	10.5
Maximum Inrush current (230V)	[A]	70	70	70	70	80	70	80
Internal fuse	[AT]	4	6.3	4	6.3	12	6.3	12
Output Specification								
Output voltage range	[VDC]	24...28		48...52			72...76	
Output current	[ADC]	6	12	3	6	12	4	8
Hold up time at full load	[ms]	30						
Over voltage protection	[% Uout]	140						
General Specification								
Operating temperature range		-25°C...70°C						
Power reduction above 50°C		2% / °C						
Storage temperature		-25°C...85°C						
Humidity		95% rel. H max.						
Switching frequency		67kHz typ.						
Efficiency		>85%						
Output voltage indicator		LED						
Isolation input - output		3'000 VAC (1 minute)						
Isolation input - case		2'000 VAC (1 minute)						
Isolation output - case		500 VAC (1 minute)						
Safety class (IEC 536)		Class 1						
Safety standards meets		IEC950 EN60950 CEs for SELV						
Conducted EMI according to		EN55022 Class B EN55011 Class B FCC-B						
Electromagnetic susceptibility EMC		EN61000-4-2 4kV / 8kV EN61000-4-3 10V / m EN61000-4-4 2kV EN61000-4-6 10V EN61000-4-8 30A / m						
Case / Protection class		Steel / IP20						
Mounting		DIN rail TS35, EN50022						

94 www.LinMot.com

Figure A.19: Datasheet of the 72 V/600 W power supply of the linear motor. Figure from [1].

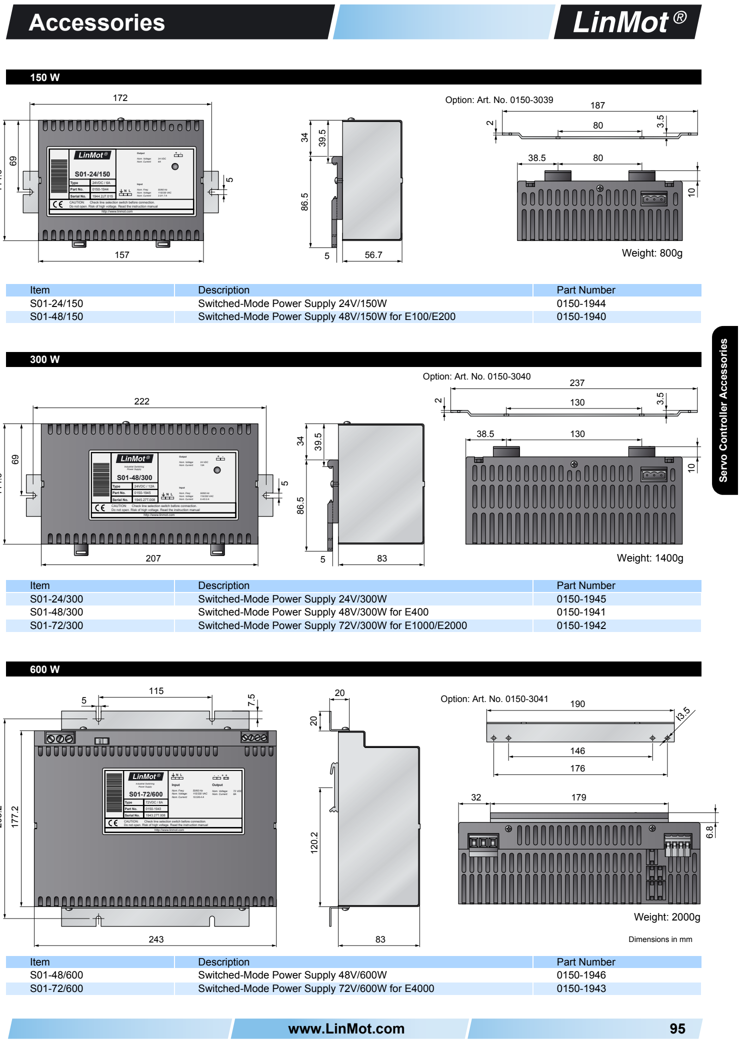

Accessories — LinMot®

150 W

Option: Art. No. 0150-3039

Weight: 800g

Item	Description	Part Number
S01-24/150	Switched-Mode Power Supply 24V/150W	0150-1944
S01-48/150	Switched-Mode Power Supply 48V/150W for E100/E200	0150-1940

300 W

Option: Art. No. 0150-3040

Weight: 1400g

Item	Description	Part Number
S01-24/300	Switched-Mode Power Supply 24V/300W	0150-1945
S01-48/300	Switched-Mode Power Supply 48V/300W for E400	0150-1941
S01-72/300	Switched-Mode Power Supply 72V/300W for E1000/E2000	0150-1942

600 W

Option: Art. No. 0150-3041

Weight: 2000g

Dimensions in mm

Item	Description	Part Number
S01-48/600	Switched-Mode Power Supply 48V/600W	0150-1946
S01-72/600	Switched-Mode Power Supply 72V/600W for E4000	0150-1943

Servo Controller Accessories

www.LinMot.com 95

Figure A.20: Datasheet of the 72 V/600 W power supply of the linear motor. Figure from [1].

Fig. A.21 presents the linear guides available in the Linmot catalog [1]. Such guides should be used if the slider is subjected to radial loads, if the rotation of the slider or the 0.5 mm gap between the slider and the stator causes inconvenience.

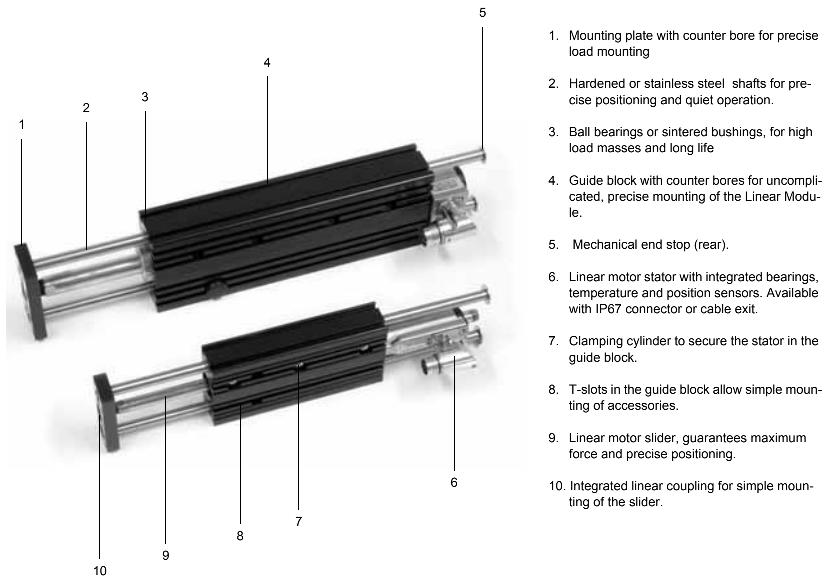

Figure A.21: Linear guides proposed in the Linmot catalog. Figure from [1].

A.2.4 Linmot Designer software: list of the parameters encoded to perform the dynamic study of the "cylinder - linear motor" combination

To perform the dynamic study of the "cylinder - linear motor" combination, a motor sizing software called "Linmot Designer" has been used (this software is available for download on the LinMot website [14]).
To study an application case with this design program, the following data must be provided:

- the global motor settings
  - the motor type and the number of motors: this specifies the short stroke SS, the maximum stroke S, the maximum peak force, the slider mass, the stator mass, etc.
    For our study, the motor type is: PO1-48X240/90X240 and there is one motor.
  - the slider mounting: regular or reversed (see Fig A.22 and A.23)
    For our study, the slider mounting is regular.
  - the cooling method: flange only or flange+fan
    For our study, a fan is used in addition to a flange.
  - the servo controller type: this automatically specifies the maximum current available for the linear motor.
    For our study, a B1100VF controller is chosen since two types of commands can be given to it. Indeed it is possible to give a current command or a slider position command.

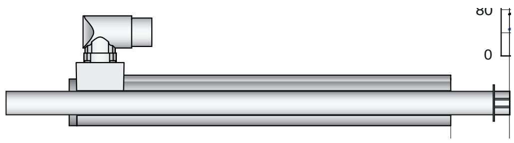

Figure A.22: "Regular" slider mounting. Figure from [1].

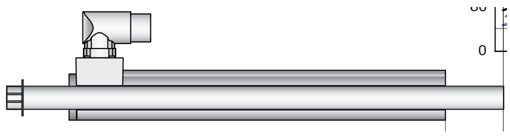

Figure A.23: "Reversed" slider mounting. Figure from [1].

- the power supply voltage.
  For our study, a 72 V*DC power supply is chosen.*
- the type and length of the cable linking the motor and the controller: indeed, the resistance of the cable can reduce the force limit.
  For our study, the cable type is K15 and the cable length is 4 m.

• the global load settings

- the start position of the motor: it can be set automatically by an auto centering function so that the motion will be symmetrical relative to the centre of the stroke range, i.e. to the Zero Position (ZP, see Fig. A.10). Indeed, according to the Linmot Designer Tutorial [3], such a motion will give the best performance.
- the mass the linear motor has to displace anytime it is actuated. Concerning the mass of the moving part of the motor, it is automatically added by the program (it is just necessary to specify whether it is the slider or the stator mass that needs to be added).
  For our study, the mass of the slider of the linear motor is automatically added by the program while the mass of the cylinder piston needs to be specified. This mass has been computed thanks to the data found in the Festo catalog and equals 243 g.
- the constant external force applied to the linear motor
  For our study, no constant external force is applied.
- the dry and viscous frictions applied to the slider
  For our study, dry friction exists in the pneumatic cylinder and it equals 10 kPa *applied to the section of the piston. Since the diameter of the piston is* 32 mm*, the friction equals* 8 N.
- the angle the linear motor presents relative to the horizontal
  For our study, this angle equals $0°$.
- the spring zero position and spring constant: these parameters have to be specified if a mechanical spring is used.
  For our study, no mechanical spring is used.

• the motor layout: "moving slider" (the slider moves while the stator is fixed, see Fig. A.24) or "moving stator" (the stator moves while the slider is fixed, see Fig. A.25).
For our study, a moving slider layout is chosen.

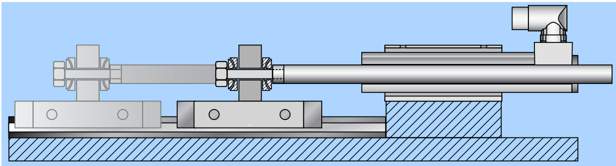

Figure A.24: "Moving slider" layout: the slider moves while the stator is fixed. Figure from [1].

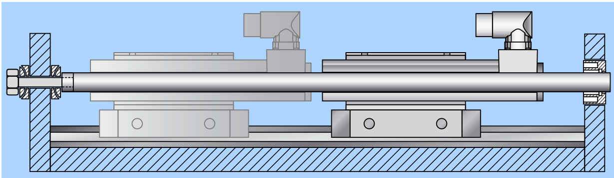

Figure A.25: "Moving stator" layout: the stator moves while the slider is fixed. Figure from [1].

Once all these data are provided to the program, the motion of the linear motor can be specified. To do so, it is segmented, i.e. it is divided into movement sections called "segments" (e.g. forward movement, backward movement, standstill). For each segment, the curve settings and the local load settings are specified:

- the curve settings
  - the curve type for the displacement, the velocity and the acceleration: sine, standstill, point to point, limited jerk or minimal jerk. According to the selected curve type, only a few of the following parameters need to be specified. Besides, it is also possible to import custom curves.
  - the segment duration
  - the covered stroke
  - the maximum velocity
  - the acceleration and deceleration
  - the maximum acceleration and maximum deceleration
  - the jerk
- the local load settings: while the global load settings are valid for any motion of the motor, the local load settings are only valid for the considered motion segment and come in addition to the global load settings.
  - the mass
    For our study, no extra mass is displaced by the motor during the considered motion segment.
  - the external force (for a regular mounting, the sign convention for the force is given in Fig. A.26)
    For our study, an external force F_{ext} is applied during the considered motion segment. It is the force applied by the pressurized gas to the cylinder piston.

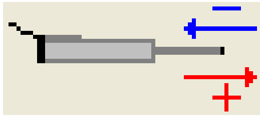

Figure A.26: Sign convention for the external force: a negative (positive) force tends to push (pull) the slider inside (out of) the stator. Figure from [3].

- the dry and viscous frictions
  For our study, no extra dry or viscous friction is applied to the slider during the considered motion segment.
- the spring start position and spring constant
  For our study, no spring is used during the considered motion segment.

If the linear motor combined with the controller and the cylinder, is not able to perform the proposed motion cycle, warnings are indicated by the Linmot Designer software. These warnings notify, for example, that the dynamic force the motor has to produce exceeds the peak force limits of the "motor - servo controller" combination.

For each application case of Table 3.2,

- a start position is specified for the motor. In practice, the slider and the cylinder piston will be connected so that only the 90 mm SS stroke of the linear motor will be used (see Section A.2.2 for a definition of the SS stroke).
  The start position is defined relatively to ZP and is thus computed as follows:

$$start\_position = 45 \text{ mm} - L, \tag{A.1}$$

  so that after a displacement of L, the slider is located at the right limit of the SS stroke (see Fig. A.10).

- the following motion cycle is studied:
  1. a forward motion of stroke L with an external force $F_{ext} = -F_{max\_statics}$ and a maximum velocity $v_{max} = 0.9$ m/s
  2. a backward motion of stroke L with an external force $F_{ext} = -F_{max\_statics}$ and a maximum velocity $v_{max} = 0.9$ m/s

The constraint on the velocity is due to the pneumatic cylinder. Indeed, according to the Festo support, a velocity larger than 0.9 m/s could damage the flexible cushioning rings/pads placed at both ends of the chosen cylinder.
The goal of the dynamic study is to approach a duration time of 0.05 s for the forward motion and the backward motion, respectively. With this target in mind, a search is done for each application case in order to find a curve type and the values of the corresponding parameters so that the motor, combined with the controller and the cylinder, would be able to perform the motion cycle.

Remark: In the software, the external force $F_{ext} = -F_{max\_statics}$ is applied continuously to the cylinder piston during the motion. However, in practice, when the cylinder piston is displaced and the actuator is pressurized (depressurized), the external force increases (decreases) and its intensity finally becomes equal to $F_{max\_statics}$ (0 N), at the end of the displacement. Hence, considering that $F_{ext} = -F_{max\_statics}$ during all the motion overestimates the real external force.

A.3 MiniTec profiles

The MiniTec company [17] proposes different types of profiles and fastening elements that can be combined to easily build structures. The MiniTec components used for the test bench are:

- 45X45 F profiles of different lengths (see Fig. A.27)
- 45 GD-Z angles (see Fig. A.28)
- Power-Lock fasteners (see Fig. A.29)
- screws, square nuts and square nuts with spring metal (see Fig. A.30)
- a thread former M8: it is used to form threads in the profile holes, in order to use Power-Lock fasteners as in the last configuration shown in Fig. A.29.

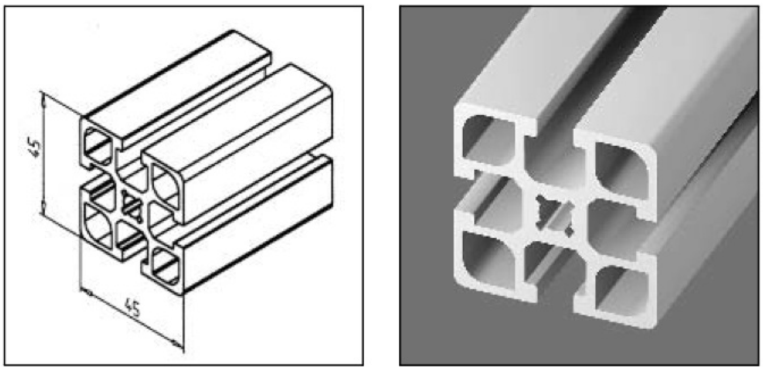

Figure A.27: 45X45 F MiniTec profiles. Figure from [2].

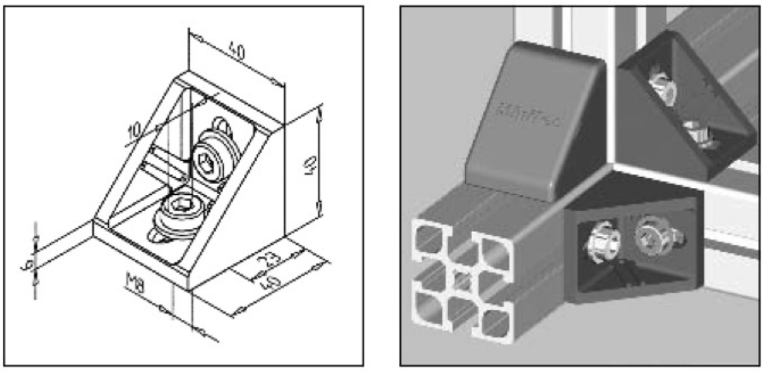

Figure A.28: 45 GD-Z MiniTec angles. Figure from [2].

Figure A.29: MiniTec Power-Lock fasteners and different ways to use them to fasten MiniTec profiles to each other. Figure from [2].

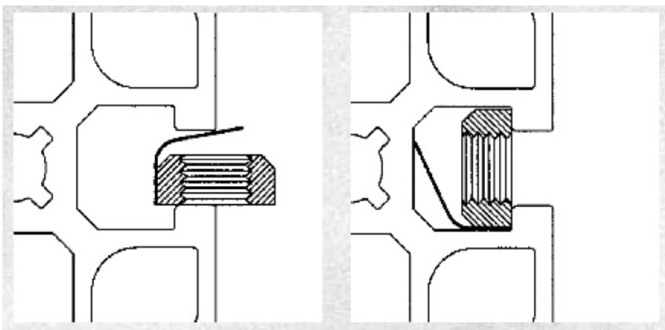

Figure A.30: View of the cross-section of a MiniTec profile in which a square nut with spring metal is inserted. Figure from [2].

A.4 National Instruments platform for measurement and control: detailed list of the components of the platform

NATIONAL INSTRUMENTS

National Instruments Belgium SA
Ikaroslaan 13 B-1930 Zaventem
Tel : 02/757.00.20 Fax : 02/757.03.11
BTW BE 445.607.706 HRB 552.093
KB 436-6252841-86

ULB
Mme Aline De Greef
Fac. Sciences Appliquées
Av. F.D. Roosevelt 50 CP165/14
1050 Bruxelles

Date 26-08-2008

Offre de prix N° 933400 - 1

Pour consulter la ou les configurations proposées, rendez-vous sur http://ni.com/advisors/retrieve.
ID de configuration : PX676261

Poste	Qté	Article	Description	Prix p/u	Remise	Prix Net
1	2	186381-02	SH68-C68-S 68-Pin VHDCI to 68-Pin. D-Type, 2m Pays d'origine : Mexico	89,00	10.00%	160,20 Eur
2	2	192061-02	SHC68-68-EPM Shielded Cable, 68-D-Type to 68 VHDCI Offset, 2 m Pays d'origine : China	109,00	10.00%	196,20 Eur
3	1	763067-01	Power Cord, 240V, 10A, Euro, Right Angle Pays d'origine : China	9,00	10.00%	8,10 Eur
4	1	776844-01	SCB-68 Noise Rejecting, Shielded I/O Connector Block Pays d'origine : Hungary	269,00	10.00%	242,10 Eur
5	1	778636-01	NI PXI-1042 8-Slot 3U Chassis with Universal AC Power Supply Pays d'origine : China	1.799,00	10.00%	1.619,10 Eur
6	1	778998-01	NI PXI-6723 32-Channel Analog Output Board Pays d'origine : Hungary	1.149,00	10.00%	1.034,10 Eur
7	1	779114-01	NI PXI-6224, M Series DAQ (32 Analog Inputs, 48 Digital I/O) with NI-DAQmx driver software. Pays d'origine : Hungary	679,00	10.00%	611,10 Eur
8	2	779475-01	SCC-68 I/O Connector with 4 SCC Module Slots Pays d'origine : Hungary	269,00	10.00%	484,20 Eur
9	1	779886-02	NI PXI-8106 Core 2 Duo 2.16 GHz Controller with Windows Vista Pays d'origine : Hungary	3.549,00	10.00%	3.194,10 Eur
10	1	960597-08	PXI 8-Slot Factory Installation Service and Extended Warranty Pays d'origine : Hungary	729,00		729,00 Eur
11	2	779302-1024	1 GB DDR2 RAM for NI 8106, NI 8105 and NI 8104 Controllers Pays d'origine : USA	219,00	10.00%	394,20 Eur
			Sous-Total			8.672,40 Eur
			Transport			100,19 Eur
			Total			8.772,59 Eur

Figure A.31: Order of the National Instruments platform for measurement and control

A.5 Detailed description of the connections between the motor controller, the motor fan and the different power supplies

Fig. A.32 explains how the controller of the linear motor has to be connected. As can be seen, the controller is connected to two power supplies: the linear motor supply (72 VDC) and the logic supply (24 VDC).

Power Supply and Grounding

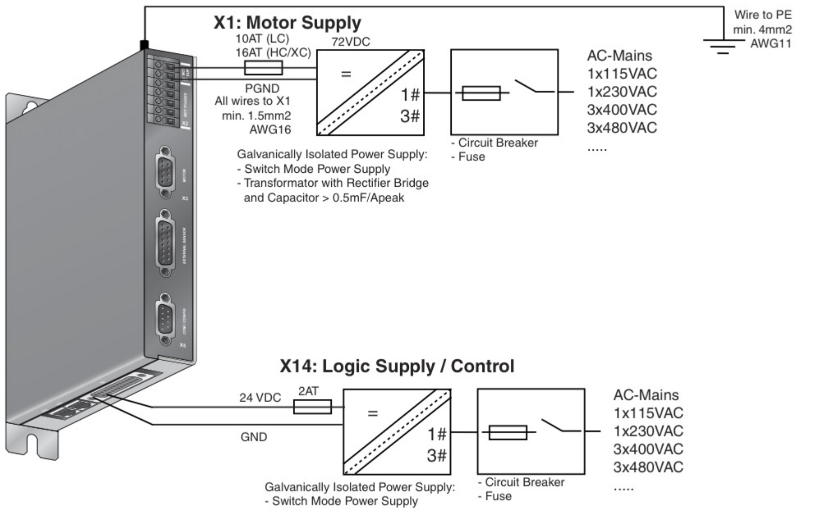

*Inside of the B1100 controller the *PWR motor GND* and *PWR signal GND* is connected together and to the GND of the controller housing. It is recommended that the *PWR motor GND* is NOT grounded at another place than inside of the controller to avoid circular currents.

In order to assure a safe and error free operation, and to avoid severe damage to system components, **all system components* must be well grounded to either a single earth or utility ground.** This includes both LinMot and all other control system components to the same ground bus.

Each system component* should be tied directly to the ground bus **(star pattern)**, rather than daisy chaining from component to component. (LinMot motors are properly grounded through their power cables when connected to LinMot controllers.)

Power supply connectors must not be connected or disconnected while DC voltage is present. Do not disconnect system components until all LinMot controllers LEDs have turned off. (Capacitors in the power supply may not fully discharge for several minutes after input voltage has been disconnected). Failure to observe these precautions may result in severe damage to electronic components in LinMot motors and/or controllers.

Do not switch Power Supply DC Voltage. All power supply switching and E-Stop breaks should be done to the AC supply voltage of the power supply. Failure to observe these precautions may result in severe damage to controller.

Figure A.32: Explanations about how to connect the motor controller to the 72 VDC motor supply and the 24 VDC logic supply. Figure from [8].

The 24 VDC logic supply was not provided with the linear motor. Hence, a 24 VDC power supply has been bought and its main characteristics are summarized in Table A.1.

24 VDC logic supply of the linear motor controller	
brand	SIEMENS
type	SITOP modular 5A 1/2phasig 6EP1 333-3BA00
output DC voltage	$24VDC \pm 1\%$
direct output current	$0 - 5$ A
power consumption (active power)	140 W
rated input voltage	$120VAC$ / $230VAC - 500VAC$, 50/60 Hz
input current at 230 V	1.2 A_{rms}
can be installed on DIN rail	yes

Table A.1: Main properties of the 24 VDC logic supply of the linear motor controller

Following the explanations of Fig. A.32, the connections between the controller, the 72 VDC motor supply, the 24 VDC logic supply, the fan and its supply have been made as shown in Fig. A.33.

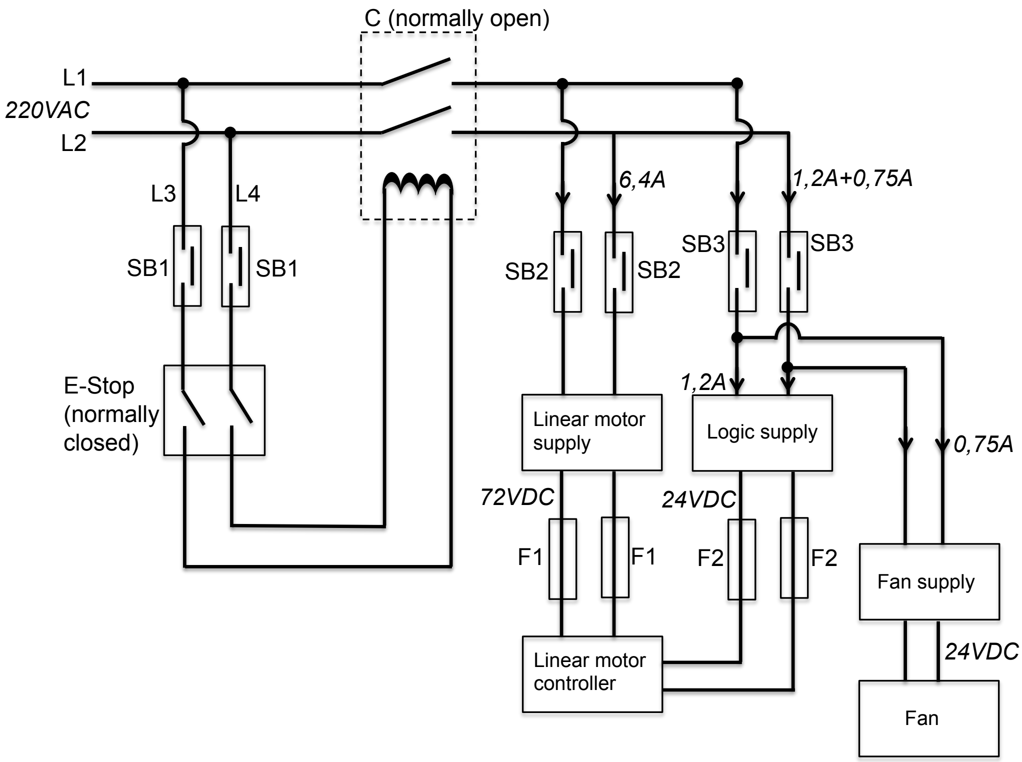

Figure A.33: Connections between the controller, the 72 VDC motor supply, the 24 VDC logic supply, the fan and its supply. "F", "SB", "L" and "C" stand for "fuse", "switching break", "line" and "contactor", respectively.

The fuses, the switching breaks, the E-Stop button, the contactor and the fan supply of the circuit have the following characteristics:

- F1 is a $10AT$ fuse[2] (as suggested by Fig. A.32) under $72VDC$ but it is able to bear $550VAC$ and $250VDC$. It protects the controller and the linear motor supply.
- F2 is a $2AT$ fuse (as suggested by Fig. A.32) under $24VDC$ but it is able to bear $550VAC$ and $250VDC$. It protects the controller and the logic supply.
- SB1 is a switching break whose limit current equals $2A$. It is under $220VAC$ but it is able to bear $440VAC$ and $60VDC$. It protects the E-stop button, which can bear up to $3A$, and the coil of the contactor C. As the contactor consumes $70VA$ and is under $220VAC$, the current in its coil equals $\frac{70VA}{220VAC} = 0.3A$. A switching break whose limit current is larger than $0.3A$ but close to 0.3 A has been looked for and the best match found is a switching break offering a limit current of $2A$.
- SB2 is a switching break whose limit current equals $10A$. It is under $220VAC$ but it is able to bear $440VAC$ and $60VDC$. It protects the linear motor supply, which consumes up to $6.4A$ (= "input current at full load ($230V$)", see Section A.2.3, in Fig. A.19). Hence, the best match found for the switching break is a limit current of $10A$.
- SB3 is a switching break whose limit current equals $2A$. It is under $220VAC$ but it is able to bear $440VAC$ and $60VDC$. It protects the logic supply and the fan supply. The logic supply consumes $1.2A$ (see Table A.1) while the fan supply consumes 0.75 A (see Table A.2). This makes $1.2\text{ A} + 0.75\text{ A} = 1.95\text{ A}$. The best match found for this switching break is a limit current of $2A$.
- An E-Stop button is combined with a contactor C so that when the E-Stop button is pressed, the contactor opens the lines L1 and L2 and the circuit is no more provided with current.
  The contactor is composed of a coil and two breaks, which are placed in the lines L1 and L2. The chosen contactor is normally open. This means that when the coil is not (is) put under voltage, the lines L1 and L2 are open (closed).
  The E-Stop button is normally closed. This means that when the E-Stop button is not (is) pressed, the lines L3 and L4 are closed (open).
  Hence, when the E-Stop button is pressed, lines L3 and L4 open, thus the coil of the contactor is no more under voltage, this involves the opening of lines L1 and L2 and the rest of the circuit is no more put under voltage.
  In the lines L1 and L2 a current of $8.35A$ runs ($6.4A$ for the linear motor supply + $1.2A$ for the logic supply + $0.75A$ for the fan supply). The E-Stop button can bear $3A$ and is thus not able to open the lines L1 and L2.
  This is why a contactor has been combined with the E-Stop. This contactor is under $220VAC$ (but is able to bear $440VAC$) and is able to open a line travelled by a current of $10A$. The E-Stop commands the opening of lines L1 and L2 but in practice, it is the contactor that opens the lines.
- The fan of the linear motor requires a supply providing $24VDC$ and $120mA$, as can be seen in Section A.2.3, in Fig. A.13. This supply is not provided with the linear motor and has been bought separately. Its characteristics are summarized in Table A.2.
- Limit switches are interesting devices to add to the test bench as they can help to increase the safety of operation of the linear motor. Indeed, as the motor has a much

[2] The notation $x\ AT$ for a fuse means that the fuse is going to blow if the current exceeds xA. "T" stands for "temporized" and means that when the current achieves the limit, the fuse is not going to blow immediately, but after a certain period of time.

24VDC fan supply	
brand	RS
type	DR-45 series 282-473
output DC voltage	$24VDC \ \pm\ 1\%$
rated output current	2 A
output rated power	48 W
input voltage range	85 $\sim$ 264 VAC or 120 $\sim$ 370 VDC, 47 $\sim$ 63 Hz
input typical AC current at 230VAC	0.75 A
can be installed on DIN rail	yes

Table A.2: Main properties of the 24VDC fan supply

larger stroke than the pneumatic cylinder, limit switches can be used to shut down the motor supply when the displacement of the motor slider risks exceeding the cylinder stroke. The limit switches used for the test bench are presented in Fig. A.34. When the metallic bar is pressed downwards (is at rest), it pushes (doesn't push) on the A button and the connection between COM and NO (normally open) (COM and NC (normally closed)) is established.

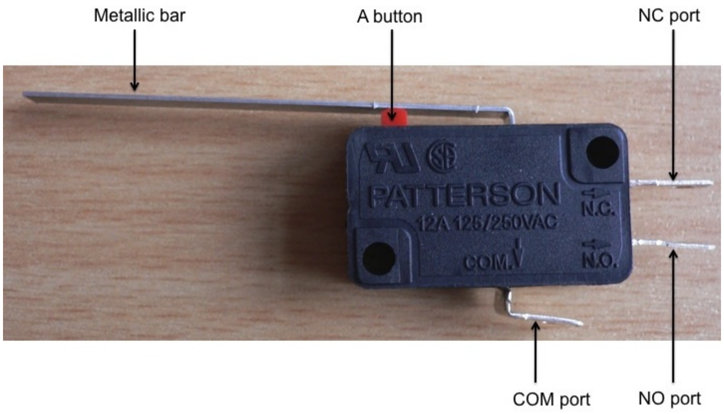

Figure A.34: Picture of the limit switches used in the test bench

The limit switches could be installed in series with the E-Stop button. Hence, if a limit switch is pressed, the circuit lines L1 and L2 open and the motor supply is shut down. Afterwards, as soon as the limit switch is no more pressed, lines L1 and L2 close and the motor supply switches on again. Since it was preferred that an external manual action was required to switch on the power again, another solution has been implemented. Indeed, as shown in Fig. A.35, the limit switches (LS1 and LS2) have been connected to a shunt itself bond (with a physical bond) to two switching breaks SB4 placed in the lines L1 and L2. When a limit switch is pressed, the shunt is put under voltage, it opens the switching breaks and this shuts the power off. A manual action is then necessary to close the SB4 switching breaks in order to put the power on again.

- Earth connectors to be fixed to DIN rails (see Fig. A.36) are placed at different locations in the circuit to allow the connection of the different components to the earth.

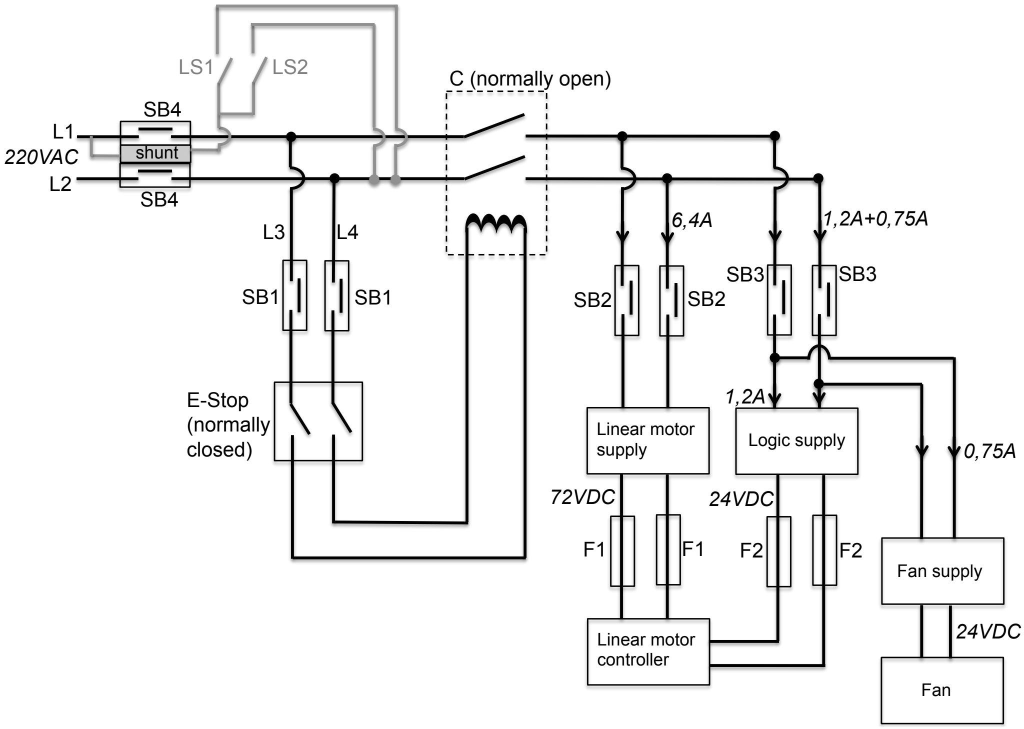

Figure A.35: Connections between the controller, the 72 VDC motor supply, the 24 VDC logic supply, the fan and its supply, the shunt and the limit switches. "F", "SB", "L", "C" and "LS" stand for "fuse", "switching break", "line", "contactor" and "limit switch", respectively.

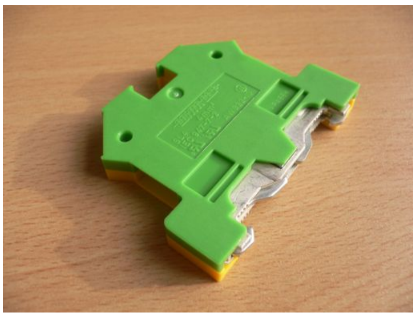

Figure A.36: Earth connector

The main characteristics of the fuses, the fuse holders, the switching breaks, the limit switches, the E-Stop button, the earth connectors, the shunt and the contactor are summarized in Tables A.3 and A.4.

fuses F1	brand: GE Power Controls part number: NIT10 current rating: $10A$ max. voltage rating ac: $550V$ max voltage rating dc: $250V$ fuse technology: T; HBC fuse type: A1
fuses F2	brand: GE Power Controls part number: NIT2 current rating: $2A$ max. voltage rating ac: $550V$ max voltage rating dc: $250V$ fuse technology: T; HBC fuse type: A1
fuse holders	brand: Cooper Bussmann part number: CM32FC current rating: $32A$ fuse type: A1 installation on DIN rails: yes
switching breaks SB1 and SB3	brand: ABB part number: S201D2 current rating: $2A$ rated voltage: $440VAC/60VDC$ tripping characteristics: type D number of poles: 1 short circuit capacity: $6kA$ installation on DIN rails: yes
switching breaks SB2	brand: ABB part number: S201D10 current rating: $10A$ rated voltage: $440VAC/60VDC$ tripping characteristics: type D number of poles: 1 short circuit capacity: $6kA$ installation on DIN rails: yes
switching breaks SB4	brand: ABB part number: S203D10 current rating: $10A$ rated voltage: $440VAC$ tripping characteristics: type D number of poles: 3 short circuit capacity: $6kA$ installation on DIN rails: yes

Table A.3: Main characteristics of the fuses, the fuse holders and the switching breaks

limit switches LS1 and LS2	brand: Patterson maximum current: $12A$ rated voltage: 125 $250VAC$
E-stop button	brand: Telemecanique part number: XAL-K174F turn to release AC current under 240V: $3A$ contact configuration: 2N/C
earth connectors	brand: RS part number: 1212.2 installation on DIN rails: yes
shunt	brand: ABB part number: S2C-A2 operating current at $230VAC$: $1A$ installation on DIN rails: yes
contactor	brand: RS part number: 135-020 contact configuration: 2 NO and 2 NC coil voltage: 50/60 Hz - $230V$ installation on DIN rails: yes

Table A.4: Main characteristics of the limit switches, the E-Stop button, the earth connectors, the shunt and the contactor

A.6 Sensors

Before the measurements of the pressure sensors are acquired by the NI PXI platform, they pass through anti-aliasing filters whose electronic circuit is presented in Fig. A.37. The characteristics of this circuit components are given in Table A.5.

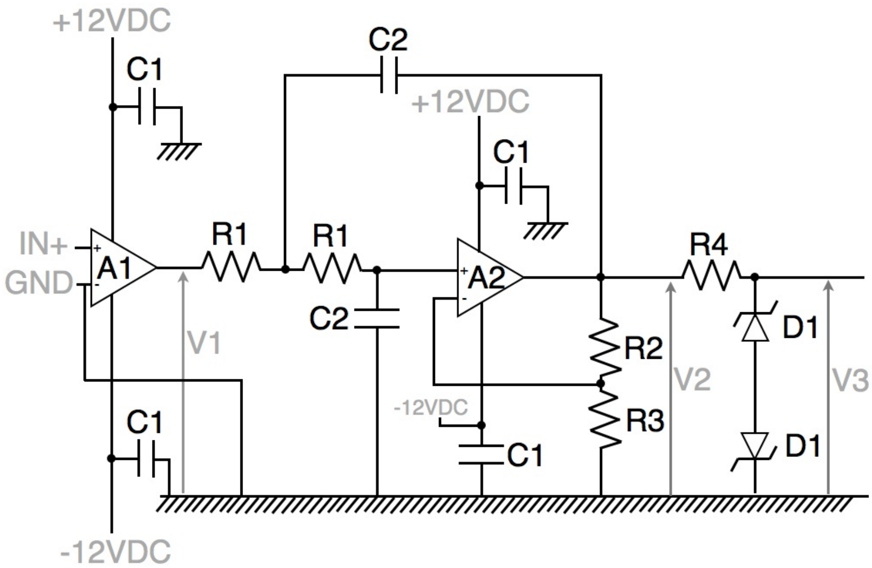

Figure A.37: Electronic circuit of the anti-aliasing filters

Component	Characteristics
A1	instrumentation amplifier AD620AN
A2	operational amplifier TLE 2061
C1	decoupling capacitor $C1 = 100\ nF$
C2	capacitor $C2 = 22\ nF$
R1	resistor $R1 = 7.15\ k\Omega$
R2	resistor $R2 = 1.21\ k\Omega$
R3	resistor $R3 = 2.05\ k\Omega$
R4	resistor $R4 = 1\ k\Omega$
D1	Zener diode maximum power $= 0.4\ W$ breakdown voltage $= 9.1V$

Table A.5: Components of the anti-aliasing circuits

The electronic cards of the anti-aliasing circuits have been manufactured as follows:

1. The electronic circuit is drawn as a block diagram with the EAGLE software.
2. According to the block diagram, the EAGLE software draws the tracks that will connect the electronic components.
3. The produced EAGLE file is provided to a numerically controlled machine.
4. A copper coated plate is placed in the numerically controlled machine.
5. The machine draws the electronic tracks by removing copper and it makes holes in the plate to allow the fixing of the electronic components.
6. The electronic components are welded on the card.

Fig. A.38 and A.39 present the EAGLE block diagrams of the anti-aliasing filter described above. Fig. A.40 and A.41 present the corresponding electronic tracks drawn by the EAGLE software.

Three anti-aliasing filters have been manufactured. Two of them correspond to Fig. A.38 and A.40 and are the filters of the pressure sensors, while the third filter corresponds to Fig. A.39 and A.41. This third filter had been dedicated to a force sensor which was finally not used. However, this filter contains a TML 10212 which is an electronic component that produces the supply voltages ($+12\ VDC$ and $-12\ VDC$) used for the instrumentation and the operational amplifiers of the three filters. This explains why this anti-aliasing filter has been kept although the force sensor is not used anymore.

The circuit controlling the solenoid valve (see Chapter 4) and the anti-aliasing filters have been placed into plastic boxes to protect them from the dust and to prevent that someone touches the electronic cards with its fingers (see Fig. A.42).

The connections between the pressure sensors, the solenoid valve and the circuit controlling it (see Chapter 4), the NI PXI platform, the supplies and the anti-aliasing filters

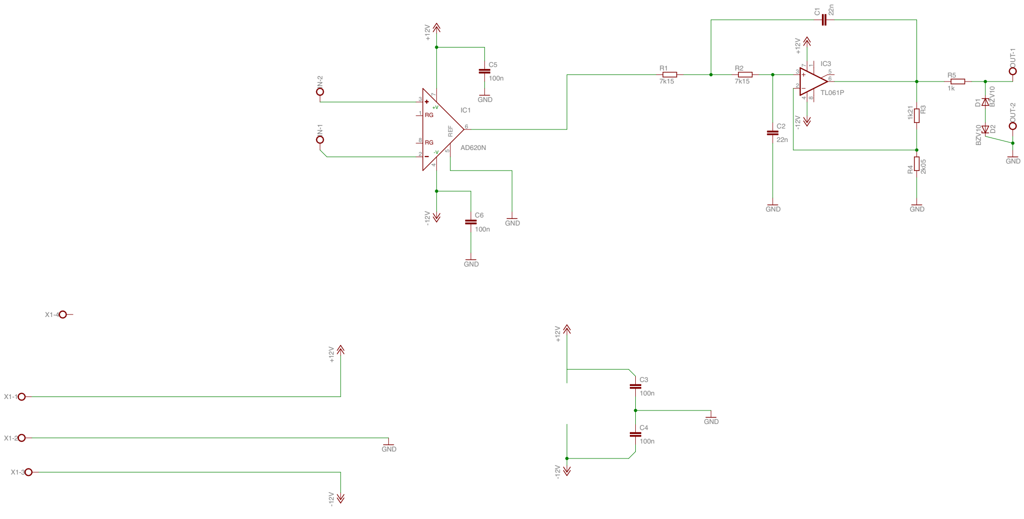

Figure A.38: Block diagram of the anti-aliasing filter, drawn with the EAGLE software

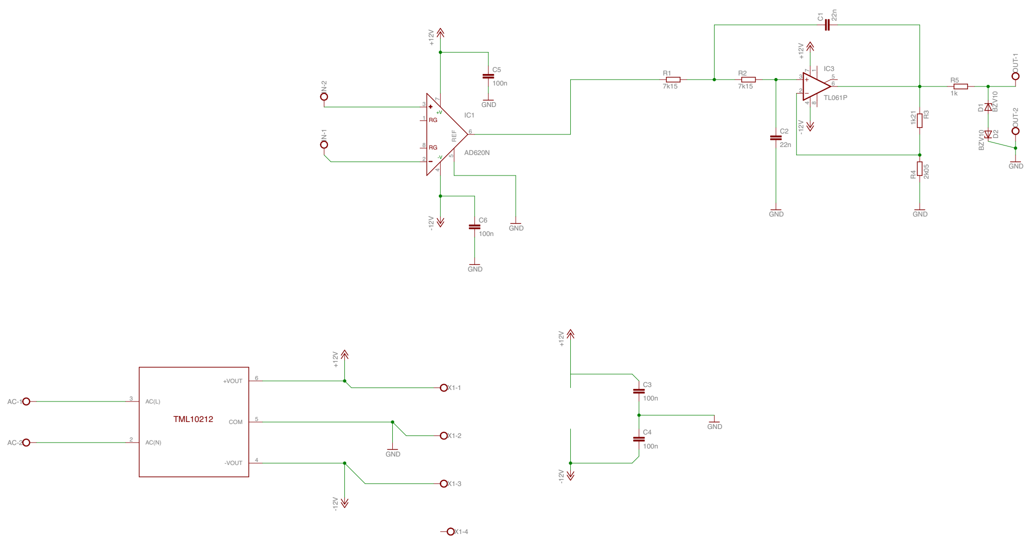

Figure A.39: Block diagram of the anti-aliasing filter, drawn with the EAGLE software. The component TML 10212 produces $+12\ VDC$ and $-12\ VDC$ voltages. These voltages are used as supply voltages for the instrumentation and the operational amplifiers.

have been organized around a central set of screw terminals (see Fig. A.43). Each element is connected to it using shielded cable and the connections between the elements are made by connecting electric wires between the different screw terminals. The shielded cables are connected to the plastic boxes thanks to female and male DB connectors.

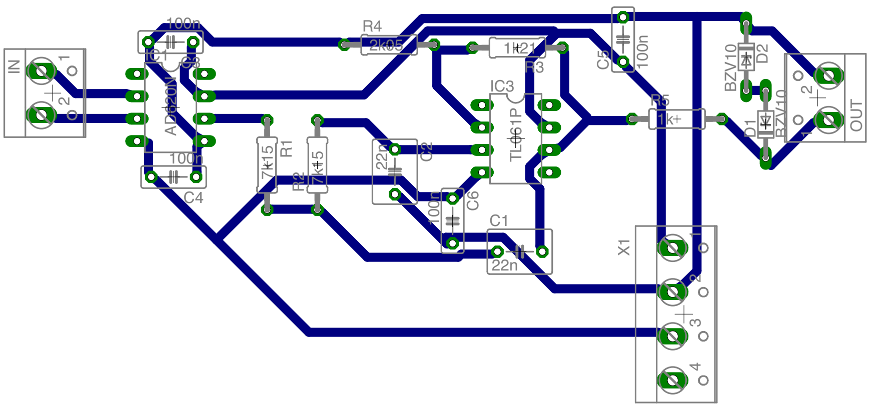

Figure A.40: Electronic tracks of the anti-aliasing filter, generated by the EAGLE software

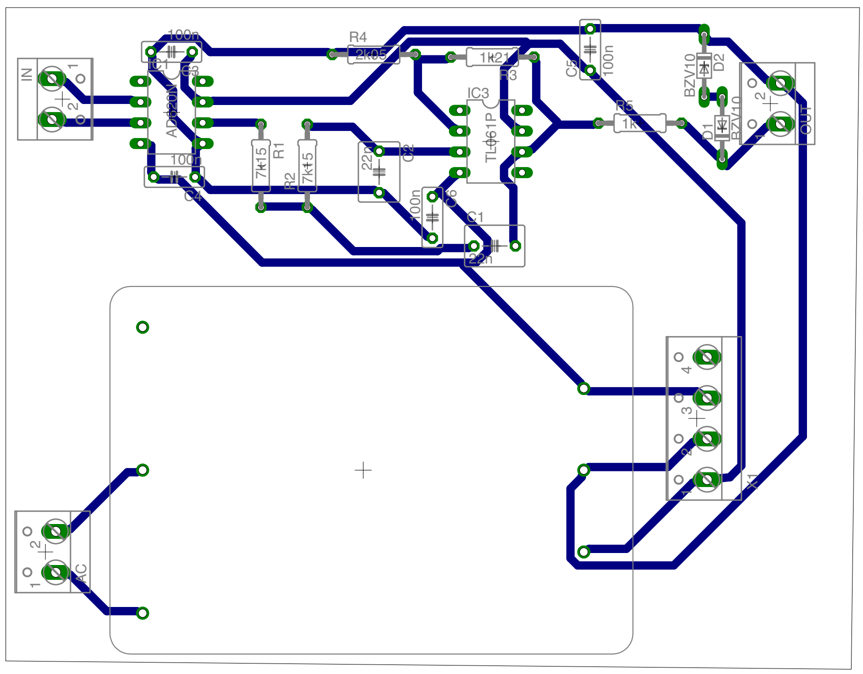

Figure A.41: Electronic tracks of the anti-aliasing filter, generated by the EAGLE software. The large rectangle component is a TML 10212 that produces $+12\,VDC$ and $-12\,VDC$ voltages. These voltages are used as supply voltages for the instrumentation and the operational amplifiers.

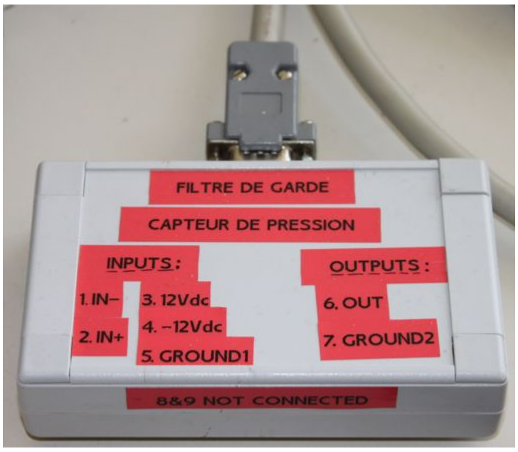

Figure A.42: Picture of one of the plastic boxes in which the electronic cards are placed.

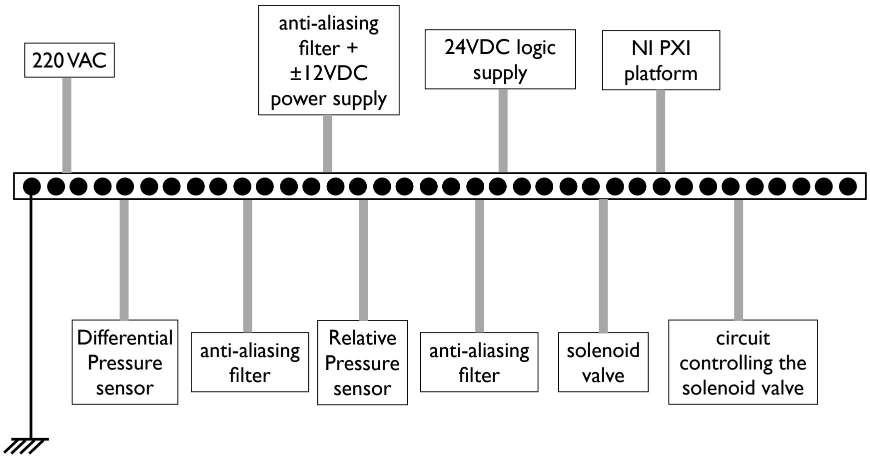

Figure A.43: Connections between the pressure sensors, the solenoid valve and the circuit controlling it, the NI PXI platform, the supplies and the anti-aliasing filters: they are organized around a central set of screw terminals. Each element is connected to it using shielded cable (= grey lines in the figure) and the connections between the elements are made by connecting electric wires between the different screw terminals. The boxe noted "anti-aliasing filter + $\pm 12\ VDC$ power supply" is the third anti-aliasing filter that contains an electronic component producing $+12\ VDC$ and $-12\ VDC$ voltages.

Appendix B

Pneumatic balloon actuators

B.1 Home-made manufacturing methods of the "Pneumatic Balloon Actuator"

As explained before (see Section 4.2.2), a Pneumatic Balloon Actuator (PBA) can be obtained simply by gluing to one another two plastic squares of different rigidities along their surrounding edge in order to form a cavity. Hence, as manufacturing these actuators seemed very easy, different methods have been tested to manufacture home-made PBAs. However, as each of the three tested methods (gluing, latex moulding and welding) presented disadvantages, it was eventually decided to look for a company to manufacture the PBAs.

B.1.1 Gluing

Principle

Two plastic squares showing different rigidities (a very flexible one and a stiffer one) are glued to one another along their surrounding edge with a glue dedicated to rubbers and plastics (a LOCTITE 406 glue). A syringe equipped with a needle is then used to pierce one of the films and to inject air in the cavity.

Results

The results were not concluding as there were leakages difficult to totally suppress by adding glue.

B.1.2 Moulding

Principle

Another idea is to mould a PBA in Latex. A mould has then been fabricated in balsa wood. The mould is made of six parts as can be seen in Fig. B.1.
Parts 1 to 5 are made of balsa while part 6 is made of polystyrene. Parts 2, 3 and 5 are glued on part 1. Before fixing part 4, a dry lubricant with PTFE is sprayed on the walls of the future cavity, on parts 1 and 4. Part 4 is then fixed to part 1 thanks to screws and nuts, as shown in Fig. B.2. Part 6 is hung in the cavity by screws and nuts (see Fig. B.3). Washers are strung on these screws and are used to position part 6 so that the distances between parts 1 and 6 and between parts 4 and 6 are different. The mould is then filled with latex and the latex dries then with the contact of air. After 36 hours, the PBA is dry and it is removed

from the mould. Latex sticks quite well to the wood but absolutely not to the polystyrene part.

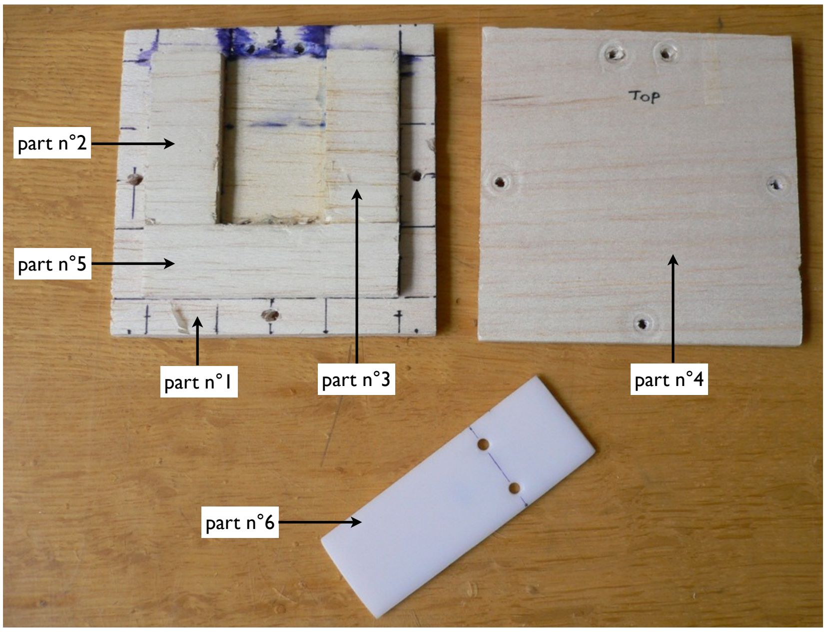

Figure B.1: Balsa mould developed to mould a PBA in Latex. Parts 2, 3 and 5 are glued on part 1.

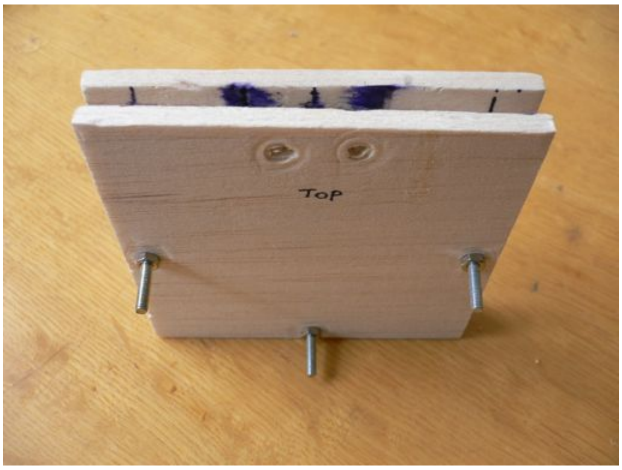

Figure B.2: Balsa mould developed to mould a PBA in Latex. The mould is here assembled without part 6.

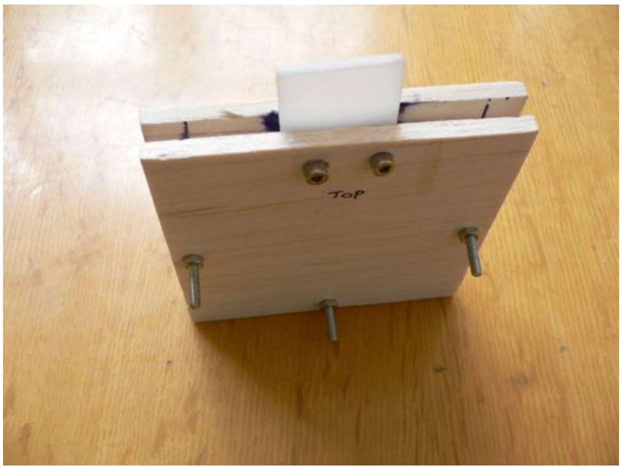

Figure B.3: Balsa mould developed to mould a PBA in Latex. The mould is here completely assembled.

Results

The achieved PBA is satisfying since it is airtight. To test it, it is clamped as a cantilever so that the size of the cavity is 30 mm $\times$ 30 mm and so that the upper cavity layer is the thinner one. Air is then injected in the cavity with a syringe equipped with a needle. As can be seen in Fig. B.4, when the PBA is pressurized, its free extremity deflects upwards but from a given pressure level, it begins to displace downwards. This bidirectional behaviour has also been noticed in [50] also for PBAs completely made of the same material.

In conclusion, the proposed moulding method allows to manufacture airtight latex PBAs. However, another manufacturing method has been looked for because the manufactured PBA does not present a channel for the air supply. Indeed, the air supply is done by piercing the latex with a needle and by injecting air with a syringe. However, to insert the latex PBA in a test bench, it would be easier to have a channel to which the air supply could be properly connected. Obtaining such a channel is difficult with this moulding method. Indeed, part 6 is used to form the cavity in the PBA and it is removed before using the PBA. However, if a narrow channel is foreseen, removing part 6 after the drying of the PBA will not be possible anymore.
The welding of plastic films, whose thicknesses are guaranteed by the supplier, is then considered in section B.1.3. Indeed, this solution can solve the drawback of the moulding method if a channel is foreseen, to which a tube can be connected for the air supply.

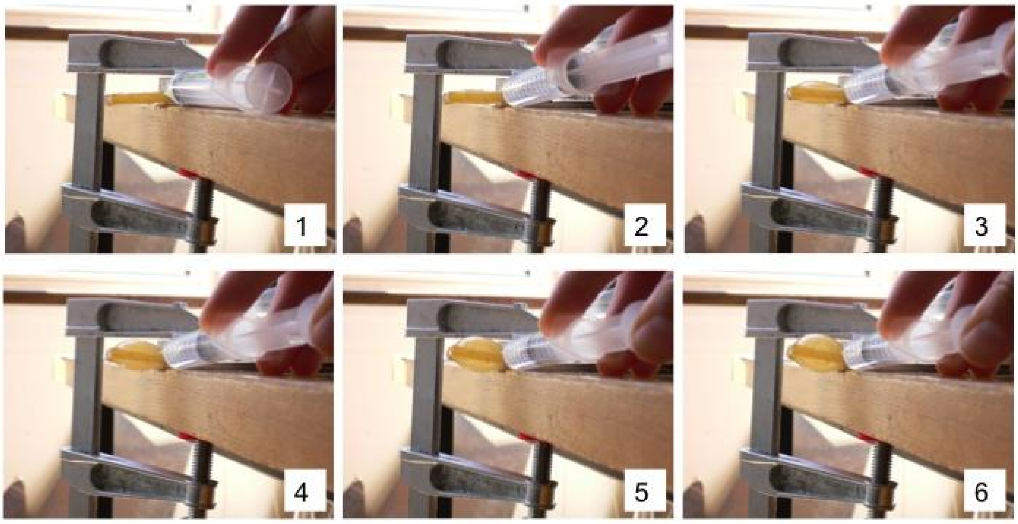

Figure B.4: Behaviour of the pressurized latex PBA. The PBA is fixed as a cantilever and air is injected in its cavity with a syringe equipped with a needle. When the PBA is pressurized, its free extremity deflects upwards but from a given pressure level, it begins to displace downwards (the downwards motion is not visible on the pictures).

B.1.3 Welding

Principle

The idea is to weld to each other two plastic films of different rigidities. To do so, films of thermoplastic elastomers (TPEs) are used. Indeed, elastomers are very elastic and will allow the inflation of the PBA while thermoplastics have the particularity to melt when they are heated [41]. Among the TPEs, it has been chosen to use thermoplastic polyurethane (TPU) since TPU exists under the form of films or sheets. Samples of TPU films of different thicknesses (50 µm, 100 µm and 200 µm) have been provided by the PLAST NEDERLAND B.V. company.
The goal is thus to weld two plastic films of different thicknesses (and thus rigidities) to each other and to obtain weldings whose shape is presented in Fig. B.5.

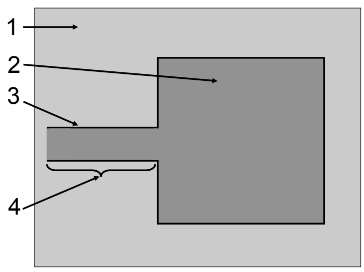

Figure B.5: PBA obtained by welding two TPU films to one another 1) TPU films 2) PBA 3) Weldings 4) Channel for the air supply

To do that, the films are pressed against an electronic card whose copper tracks are travelled by a current. The heating of the tracks involves then the melting and the welding of the films.
This card has been manufactured by lithography and Fig. B.6 presents the shape of its copper tracks. Electrodes are connected to points Z and Z' and all the copper tracks have the same thickness. Once the weldings are made, the TPU films are cut along the welded edges and a PBA is obtained.

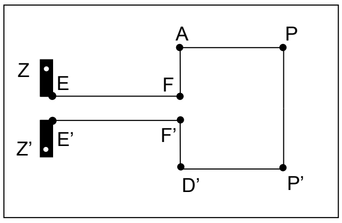

Figure B.6: Drawing of the electronic card used to manufacture PBAs by welding TPU films to each other. All the copper tracks have the same thickness.

Results

In practice, achieving a uniform welding is not easy and several trials are necessary before obtaining an airtight PBA.
<u>Remark</u>: A soldering iron has also been tested to weld two plastic films to one another but it is delicate to obtain a uniform welding of good quality with this method. Indeed, holes are made in the films if the soldering iron is pressed for too long on them.

B.2 PBA developed by the PRONAL company

Fig. B.7 shows the PBAs developed by the PRONAL company.

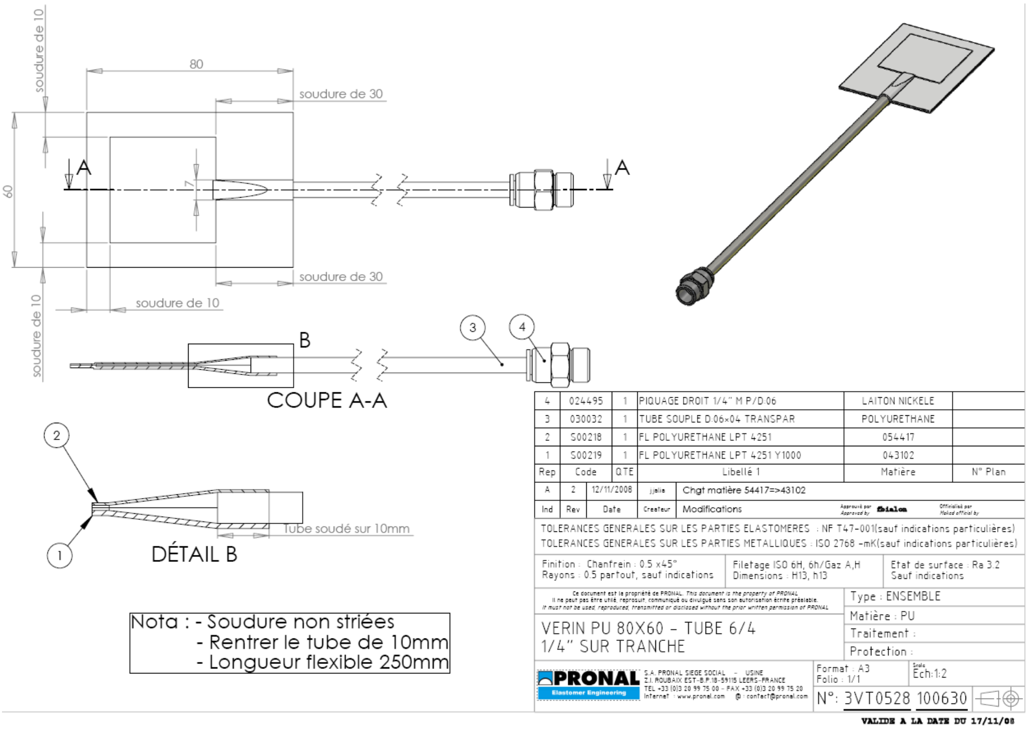

Figure B.7: Drawing of the PBA proposed by the PRONAL company. The dimensions of the cavity are 40 mm $\times$ 40 mm.

B.3 Particularities of the test bench

The relative and differential pressure sensors used to measure the pressure inside the PBAs are integrated into the fluidic circuit presented in Fig. B.8. This circuit is composed of the pneumatic cylinder chamber, the flexible fluidic actuator to be studied, the pressure sensors, a solenoid valve and the fittings and tubes connecting all these components. Table B.1 gives a description of the components of this fluidic circuit.

The solenoid valve is a 2/2-way valve presenting two pressure ports; when it is open/closed, the ports are/are not connected. The solenoid valve is normally closed. This means that when it is not powered, it is closed. On the other hand, as soon as power is supplied, it commutes and opens itself. To control the closing/opening of the valve with the NI PXI platform (see Section 3.5.2), the electronic circuit presented in Fig. B.9 has been built. *NI GND* and *NI command* are signals generated by the NI PXI platform:

- $NI\ GND = 0$ V.
- $NI\ command = 0$ V or 2 V. When $NI\ command = 2$ V ($NI\ command = 0$ V), the potential of point A is set to 0 V (24 V) and the solenoid valve sees a potential difference

of 24 V (0 V) between its terminals A and B, it is thus supplied (not supplied) and it opens itself or stays open (it closes itself or stays closed).

Remark: The electronic card of the circuit controlling the solenoid valve has been hand-made: the components have been welded on a board already presenting a network of parallel and perpendicular copper tracks.

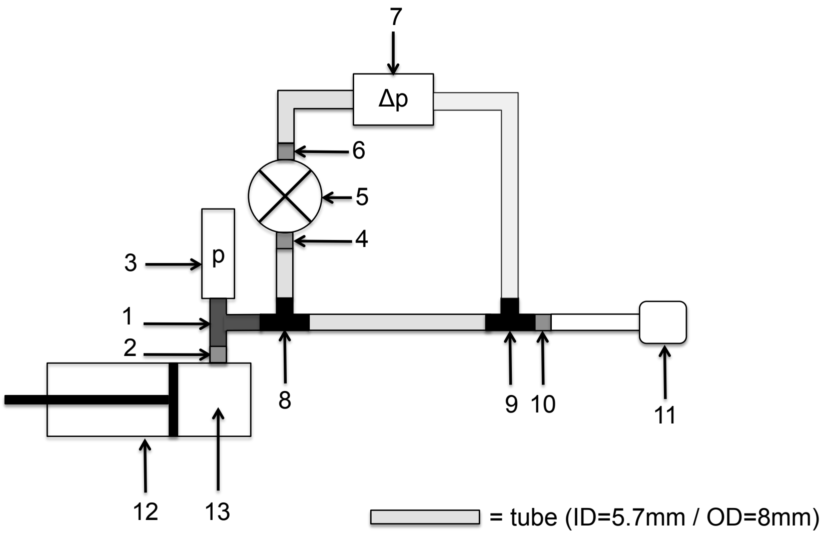

Figure B.8: Fluidic circuit implemented to study the PBAs: 1) threaded T-fitting 2) double nipple 3) relative pressure sensor 4) push-in fitting 5) solenoid valve 6) push-in fitting 7) differential pressure sensor 8) multiple distributor (one threaded fitting and two push-in fittings) 9) multiple distributor (one threaded fitting and two push-in fittings) 10) sleeve 11) PBA 12) pneumatic cylinder 13) pneumatic cylinder chamber. The light grey areas represent the tubes used to link the circuit components: ID=inner diameter and OD=outer diameter. All the fittings are equipped with seals.

Components of the fluidic circuit implemented to study the PBAs	
Component	Description
1) threaded T-fitting	brand: Festo type: NPFB - T - 3G14 - F pressure ports: G1/4 female + G1/4 female + G1/4 female
2) double nipple	brand: Festo type: NPFB - D - G18 - G14 - M pressure ports: G1/4 male + G1/8 male
3) $0-1$ *bar* relative pressure sensor	see Table 3.7 pressure port: G1/4 male
4) and 6) push-in fittings	brand: Festo type: QS - G1/8 - 8 pressure ports: G1/8 male + push-in fitting for tubes with OD = 8 mm
5) solenoid valve	brand: Burkert type: 2/2-way valve, normally closed / number: 126091 pressure ports: G1/8 female + G1/8 female
7) $0-10$ *mbar* differential pressure sensor	see Table 3.8 pressure ports: Φ 6.6 X 11, for flexible tubes with ID = 6 mm
8) and 9) multiple distributors	brand: Festo type: QSLV2 - G1/4 - 8 pressure ports: G1/4 male + 2 push-in fittings for tubes with OD = 8 mm
10) sleeve	brand: Festo type: NPFB - S - 2G14 - F pressure ports: G1/4 female + G1/4 female
11) PBA	pressure port: G1/4 male
12) pneumatic cylinder	pressure port: G1/8 female
tubes	brand: Festo type: PUN - 8 - SI - 25 - CB ID = 5.7 mm and OD = 8 mm
seals	already provided with the fittings or ordered separately and added to the fittings types of the ordered Festo seals: OL - 1/8 and OL - 1/4

Table B.1: Description of the components of the fluidic circuit implemented to study the PBAs. The numbers make reference to Fig. B.8.

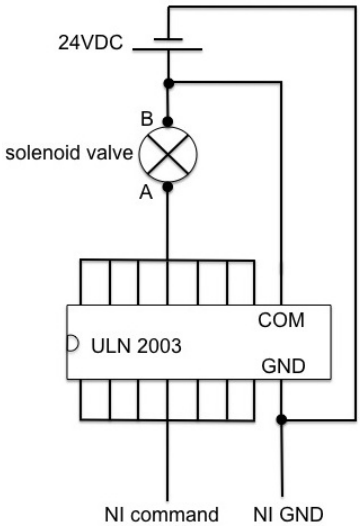

Figure B.9: Electronic circuit allowing to control the closing/opening of the solenoid valve with the NI PXI platform. This platform generates the $NI\ GND$ and $NI\ command$ signals. $NI\ GND = 0$ V and $NI\ command = 0$ V or 2 V. When $NI\ command = 2$ V ($NI\ command = 0$ V), the potential of point A is set to 0 V (24 V) and the solenoid valve sees a potential difference of 24 V (0 V) between its terminals A and B, it is thus supplied (not supplied) and it opens itself or stays open (it closes itself or stays closed).

Appendix C

List of Publications

Journal papers

- Aline De Greef, Pierre Lambert and Alain Delchambre. Towards Flexible Medical Instruments: Review of Flexible Fluidic Actuators. *Precision Engineering*, 33: 311-321, October 2009.
- Marie Blondeau, Aline De Greef, Pierre-Alexis Douxchamps, Benjamin Genêt, Marc Haelterman, Cyrille Lenders, Erwan Leroy, Pascal Nardone, Vincent Raman, Aliénor Richard and Frédéric Robert. Apprentissage par projet : Réalisation d'une éolienne urbaine en matériaux de récupération. *J3EA*, 8, 2009.

Proceedings of conferences

- Thomas Delwiche, Laurent Catoire, Michel Kinnaert and Aline De Greef. Experimental study of position-position and force-position control methods in teleoperation. In *Proceedings of the "25th Benelux Meeting on Systems and Control"*, pp108, 13-15 March 2006, Heeze, The Netherlands, ISBN-10 90-386-2558-8 ISBN-13.
- Aline De Greef, Thomas Delwiche, Laurent Catoire and Michel Kinnaert. Experimental study of position-position and force-position control methods in teleoperation. In *Proceedings of Mechatronics 2006 - 4th IFAC - Symposium on Mechatronics Systems*, pp 301-306, 12-14 September 2006, Heidelberg, Germany.
- Aline De Greef, Pierre Lambert and Alain Delchambre. A Minimally Invasive Surgery Actuator Based on a Flexible and Inflatable Structure. In *Proceedings of the First Annual symposium of the IEEE/EMBS Benelux Chapter*, 7-8 December 2006, Brussels, Belgium.
- Thierry Leloup, Aline De Greef, Sylvie Bantuelle, Wissam El Kazzi, Guy Mannaert, Nadine Warzée, Frédéric Schuind and Alain Delchambre. Design of an Articulated Mini-Fixation Device for Proximal Interphalangeal Joint Finger Fractures. In *Proceedings of the Annual Symposium of the IEEE/EMBS Benelux Chapter*, 6-7 December 2007, Heeze, The Netherlands.
- Marie Blondeau, Aline De Greef, Pierre-Alexis Douxchamps, Benjamin Genêt, Marc Haelterman, Cyrille Lenders, Erwan Leroy, Pasquale Nardone, Vincent Raman, Aliénor Richard and Frédéric Robert. Apprentissage par projet : Réalisation d'une éolienne urbaine en matériaux de récupération. *Proceedings of the "7ème Colloque sur*

l'Enseignement des Technologies et des Sciences de l'Information et des Systèmes - CETSIS 08", 27-29 October 2008, Brussels, Belgium.

- Patricia Van Dale, Aline De Greef, Cyrille Lenders and Nadine Warzée. Biomedical engineer and phlebologist: a midship frame. In *International Angiology - Proceedings of the XVI World Congress of the Union Internationale de Phlebologie (31 August - 4 September 2009)*, 28: 138, 2009.

- Aline De Greef, Pierre Lambert, Thomas Delwiche, Cyrille Lenders, Bruno Tartini and Alain Delchambre. Flexible Fluidic Actuators: Determining Force and Position Without Force or Position Sensors. In *Proceedings of the IEEE ISAM2009 conference*, 17-20 November 2009, Suwon, Korea

Miscellaneous

- Aline De Greef. *Etude d'un actionneur à structure flexible et gonflable*, DEA, Université Libre de Bruxelles, 2006.

- Aline De Greef, Pierre Lambert and Alain Delchambre. Les actionneurs fluidiques flexibles : caractérisation et application à la mesure de force sans capteurs. poster presentation at *7èmes Journées Nationales de la Recherche en Robotique JNRR'09*, 4-6 November 2009, Sologne, France.

Bibliography

[1] Industrial linear motors (edition 14) - linmot catalog.

[2] Profile system - minitec catalog.

[3] Tutorial linmot designer 1.5, 2006.

[4] European course on laparoscopic surgery - solid organs - new technology, university hospital saint-pierre, brussels, belgium, 2007.

[5] Precision linear actuators - danaher motion catalog, 2007.

[6] The lee company - website - http://www.theleeco.com/leeweb2.nsf, 2008.

[7] Modular spindle drives - maxon motor catalog, 2008.

[8] Servo controller installation guide (version 1.2/ro/june 2008) - linmot guide, 2008.

[9] Airpot corporation - website - http://www.airpot.com/, 2010.

[10] Danaher motion - website - http://www.danahermotion.com/, 2010.

[11] Design-expert 8 - website - http://www.statease.com/dx8descr.html, 2010.

[12] dspace - website - http://www.dspace.com/ww/en/pub/start.cfm, 2010.

[13] Kern & sohn gmbh - website - http://www.kern-sohn.com/, 2010.

[14] Linmot - website - http://www.linmot.com/, 2010.

[15] Lm guide actuator (model kr) - thk catalog, 2010.

[16] Maxon motor - website - http://www.maxonmotor.com/, 2010.

[17] Minitec - website - http://www.minitec.co.uk/, 2010.

[18] National instruments - website - http://www.ni.com/, 2010.

[19] Newport corporation - website - http://www.newport.com/, 2010.

[20] Pronal elastomer engineering - website - http://www.pronal.com/, 2010.

[21] Thk - website - http://www.thk.com/, 2010.

[22] Arthur W. Adamson and Alice P. Gast. *Physical Chemistry of Surfaces*. John Wiley and Sons, 6^{th} edition, 1997.

[23] C. Anthierens. *Conception d'un micro robot à actionneur asservi électropneumatique pour l'inspection intratubulaire*. PhD thesis, Institut National des Sciences Appliquées de Lyon, 1999.

[24] T. Belèndez, M. Pèrez-Polo, C. Neipp, and A. Belèndez. Numerical and experimental analysis of large deflections of cantilever beams under a combined load. *Phys. Scr.*, T118:61–65, 2005.

[25] A. M. Bertetto and M. Ruggiu. A novel fluidic bellows manipulator. *J. Robotics Mechatronics*, 16(6):604–612, 2004.

[26] P. Beyl, B. Vanderborght, R. Van Ham, M. Van Damme, R. Versluys, and D. Lefeber. Compliant actuation in new robotic applications. In *Proceedings of the NCTAM06 – 7th National Congress on Theoretical and Applied Mechanics, DVD*, 29-30 May 2006.

[27] N.-Q. Cao. Master's thesis - "miniaturisation de muscles artificiels". Master's thesis, Université libre de Bruxelles, 2009.

[28] M. C. Cavusoglu, I. Villanueva, and F. Tendick. Workspace analysis of robotic manipulators for a teleoperated suturing task. In *Proceedings of the IEEE/RSJ International Conference on Intelligent Robots and Systems (IROS 2001), Maui, HI*, volume 4, pages 2234–2239, October 29-November 3 2001.

[29] F. Daerden. *Conception and realization of Pleated Pneumatic Artificial Muscles and their use as Compliant Actuation Elements*. PhD thesis, Vrije Universiteit Brussel, 1999.

[30] F. Daerden and D. Lefeber. The concept and design of pleated pneumatic artificial muscles. *International Journal of Fluid Power*, 2(3):41–50, 2001.

[31] F. Daerden and D. Lefeber. Pneumatic artificial muscles: actuators for robotics and automation. *Eur. J. Mech. Env. Eng.*, 47(1):10–21, 2002.

[32] F. Daerden, D. Lefeber, B. Verrelst, and R. Van Ham. Pleated pneumatic artificial muscles: Compliant robotic actuators. In *Proceedings of the IEEE/RSJ International Conference on Intelligent Robots and Systems (IROS 2001), Maui, Hawaii, October-November 2001*, pages 1958–1963, 2001.

[33] R. J. Damiano, H. A. Tabaie, M. J. Mack, J. R. Edgerton, C. Mullangi, W. P. Graper, and S. M. Prasad. Initial prospective multicenter clinical trial of robotically-assisted coronary artery bypass grafting. *The Annals of Thoracic Surgery*, 72:1263–9, 2001.

[34] M. De Volder, J. Peirs, D. Reynaerts, J. Coosemans, R. Puers, O. Smal, and B. Raucent. Production and characterization of a hydraulic microactuator. *J. Micromech. Microeng.*, 15(7):15–21, 2005.

[35] S. Dohta, Y. Ban, and H. Matsushita. Application of a flexible strain sensor to a pneumatic rubber hand. In *Proceedings of the FLUCOME 2000 : the 6th Triennal International Symposium on Fluid Control, Measurement and Visualization, Sherbrooke, Canada, CD-ROM*, August 2000.

[36] E. Dombre, M. Michelin, P. Poignet, P. Bidaud, G. Morel, D. Sallé, P. Médéric, P. Gravez, M. Karouia, and N. Bonnet. Projet marge: Modélisation, apprentissage et reproduction du geste endochirurgical. In *Actes des Journées ROBEA: Journées Bilan du Programme Interdisciplinaire ROBEA'02, Toulouse, France*, pages 47–51, 24-25 October 2002.

[37] K. Donovan, C. Penninger, A. Plinta, and A. Rashid. Microfingers for micromanipulation, 2004.

[38] Festo. Fluidic muscle dmsp, with press-fitted connections / fluidic muscle mas, with screwed connections (festo catalog), 2005.

[39] F. Frey. *Traité de Génie Civil de l'école polytechnique de Lausanne : Analyse des structures et milieux continus (volume 2).* 2000.

[40] Aline De Greef, Pierre Lambert, and Alain Delchambre. Towards flexible medical instruments: Review of flexible fluidic actuators. *Precis. Eng.*, 33:311–321, October 2009.

[41] C. A. Harper. *Handbook of Plastics, Elastomers and Composites.* 1992.

[42] Y. Hayama. Flexible actuator, patent: Publication number jp2004181569, 2004.

[43] S. Hirai, T. Masui, and S. Kawamura. Prototyping pneumatic group actuators composed of multiple single-motion elastic tubes. In *Proceedings of the IEEE International Conference on Robotics and Automation, Seoul, Korea*, volume 4, pages 3807–3812, May 2001.

[44] L. L. Howell. *Compliant Mechanisms.* Interscience, July 2001.

[45] K. Ikuta, H. Ichikawa, K. Suzuki, and T. Yamamoto. Micro hydrodynamic actuated mutiple segments catheter for safety minimally invasive therapy. In *Proceedings of the 2003 IEEE International Conference on Robotics and Automation, Taipei, Taiwan*, pages 2640–2645, 14-19 September 2003.

[46] P. Joli and Z.-Q. Feng. Modélisation adaptée pour une simulation interactive d'un actionneur hydraulique. In *7ème colloque National en Calcul des Structures, Gies, France*, may 2005.

[47] H.-W. Kang, I. H. Lee, and D.-W. Cho. Development of a micro-bellows actuator using micro-stereolithography technology. *Microe. Eng.*, 83:1201–1204, 2006.

[48] G. K. Klute. *Artificial Muscles: Actuators for Biorobotic Systems.* PhD thesis, University of Washington, 1999.

[49] S. Konishi, F. Kawai, and P. Cusin. Thin flexible end-effector using pneumatic balloon actuator. *Sensors and Actuators A*, 89:28–35, 2001.

[50] S. Konishi, M. Nokata, O. C. Jeong, S. Kusuda, T. Sakakibara, M. Kuwayama, and H. Tsutsumi. Pneumatic micro hand and miniaturized parallel link robot for micro manipulation robot system. In *Proceedings of the 2006 IEEE International Conference on Robotics and Automation, Orlando, Florida*, pages 1036–1041, May 2006.

[51] S. Konishi, M. Nokata, O.C. Jeong, T. Sakakibara, S. Kusuda, M. Kuwayama, and H. Tsutsumi. Merging micro and macro robotics toward micro manipulation for biomedical operation. In *Proceedings of the 36th International Symposium on Robotics (ISR 2005)*, 2005.

[52] S. Konishi, S. Sawano, S. Kusuda, and T. Sakakibara. Fluid-resistive bending sensor compatible with a flexible pneumatic balloon actuator. *J. Robotics Mechatronics*, 20(3):436–440, 2008.

[53] M. Lazeroms, A. La Haye, W. Sjoerdsma, W. Scheurs, W. Jongkind, G. Honderd, and C. Grimbergen. A hydraulic forceps with force-feedback for use in minimally invasive surgery. *Mechatronics*, 6(4):437–446, 1996.

[54] Y. K. Lee and I. Shimoyama. A mutli-channel micro valve for micro pneumatic artificial muscle. In *Proceedings of the Fifteenth IEEE International Conference on Micro Electro Mechanical Systems, Las Vegas, USA*, pages 702–705, 2002.

[55] Y.-W. Lu and CJ Kim. Characterization of balloon-jointed micro-fingers. In *Proceedings of the 2003 ASME International Mechanical Engineering Congress and Exposition (IMECE), Washington DC, USA*, pages 311–316, 15-21 November 2003.

[56] W. McMahan, B. A. Jones, V. Chitrakaran, M. Csencsits, M. Grissom, M. Pritts, C. D. Rahn, and I. D. Walker. Field trials and testing of the octarm continuum manipulator. In *Proceedings of the International Conference on Robotics and Automation, Orlando, Florida*, pages 2336–2341, May 2006.

[57] A. Menciassi, M. Quirini, and P. Dario. Microrobotic technologies in endoluminal applications. In *presentation at the IARP - IEEE / RAS - EURON Joint Workshop on "Micro and Nano Robotics", Paris, France*, 23-24 October 2006.

[58] J. M. Morrison. Remotely controlled arm, patent: Publication number gb2100826, 1983.

[59] Y. Muyari, Y. Haga, T. Mineta, and M. Esashi. Development of hydraulic suction type active catheter using super elastic alloy tube. In *Proceedings of the 20th Sensor Symposium*, pages 57–60, 2003.

[60] T. Noritsugu, M. Kubota, and S. Yoshimatsu. Development of pneumatic rotary soft actuator made of silicone rubber. *J. Robotics Mechatronics*, 13(1):17–22, 2001.

[61] D. J. O'Brien and D. M. Lane. 3d force control system design for a hydraulic parallel bellows continuum actuator. In *Proceedings of the 2001 IEEE International Conference on Robotics and Automation, Seoul, Korea*, pages 2375–2380, 21-26 May 2001.

[62] J. Ok, M. Chu, and CJ Kim. Pneumatically driven microcage for micro-objects in biological liquid. In *Proc. of IEEE MEMS*, pages 459–563, 17-21 January 1999.

[63] J. Peirs, J. Clijnen, D. Reynaerts, H. Van Brussel, P. Herijgers, B. Corteville, and S. Boone. A micro optical force sensor for force feedback during minimally invasive robotic surgery. *Sensors and Actuators A*, 115:447–455, 2004.

[64] G. Picinbono and J.-C. Lombardo. Extrapolation: a solution for force feedback? In *Virtual Reality and Prototyping, Laval, France*, pages 117–125, June 1999.

[65] P. Poignet and G. Poisson. La conception de robots pour l'assistance aux gestes médicaux et chirurgicaux. In *5èmes journées nationales de la recherche en robotique, Guidel, Morbihan, France*, October 2005.

[66] C. Prelle. *Contribution au contrôle de la compliance d'un bras de robot à actionnement électropneumatique.* PhD thesis, Institut National des Sciences Appliquées de Lyon, 1997.

[67] A. Ruzzu, K. Bade, J. Fahrenberg, and D. Maas. Positioning system for catheter tips based on an active microvalve system. *J. Micromech. Microeng.*, 8:161–164, 1998.

[68] D. Salle. *Conception Optimale d'Instruments Robotisés à Haute Mobilité pour la Chirurgie Mini-Invasive.* PhD thesis, Université Paris 6, 2004.

[69] S. Schulz, C. Pylatiuk, and G. Bretthauer. A new ultralight anthropomorphic hand. In *Proceedings of the 2001 IEEE International Conference on Robotics and Automation (ICRA 2001), Seoul, Korea*, volume 3, pages 2437–2441, 2001.

[70] S. T. Smith and R. M. Seugling. Sensor and actuator considerations for precision, small machines. *Precis. Eng.*, 30:245–264, 2006.

[71] K. Suzumori. Elastic materials producing compliant robots. *Robotics and Autonomous Systems*, 18:135–140, 1996.

[72] K. Suzumori, S. Iikura, and H. Tanaka. Development of flexible microactuator and its applications to robotic mechanisms. In *Proceedings of the 1991 IEEE International Conference on Robotics and Automation, Sacramento, California, USA*, volume 2, pages 1622–1627, April 1991.

[73] K. Suzumori, S. Iikura, and H. Tanaka. Flexible microactuator for miniature robots. In *Proceedings of the 1991 IEEE Micro Electro Mechanical System, Nara, Japan*, pages 204–209, 30 January - 2 February 1991.

[74] K. Suzumori, S. Iikura, and H. Tanaka. Applying a flexible microactuator to robotic mechanisms. *IEEE Control Systems Magazine*, 12:21–27, 1992.

[75] K. Suzumori, A. Koga, and R. Haneda. Microfabrication of integrated fmas using stereo lithography. In *Proceedings of the 1994 IEEE Micro Electro Mechanical System, Oiso, Japan*, pages 136–141, January 1994.

[76] K. Suzumori, A. Koga, F. Kondo, and R. Haneda. Integrated flexible microactuator systems. *Robotica*, 14:493–498, 1996.

[77] K. Suzumori, T. Maeda, H. Wantabe, and T. Hisada. Fiberless flexible microactuator designed by finite-element method. *IEEE-ASME Trans. Mechatron.*, 2, issue 4, December 1997.

[78] K. Suzumori, T. Matsumaru, and S. Iikura. Elastically deformable fluid actuator, us patent 4,976,191, 11 December 1990.

[79] P. Taillard. Guide de dimensionnement - la production d'énergie pneumatique. *Technologie*, (110):21–25, novembre - décembre 2000.

[80] K. Takemura, S. Yokota, and K. Edamura. Development and control of a micro artificial muscle cell using electro-conjugate fluid. *Sensors and Actuators A*, Article in press, 2006.

[81] G. Thomann. *Contribution à la chirurgie minimalement invasive: conception d'un coloscope intelligent.* PhD thesis, National Institute of Applied Sciences in Lyon, 2003.

[82] L. Toledo, D. Gossot, S. Fritsch, Y. Revillon, and C. Reboulet. Etude des forces subies et de l'espace de travail des instruments de chirurgie endoscopique. *Annales de Chirurgie*, 53(7), 1999.

[83] B. Verrelst. *A dynamic walking biped actuated by pleated pneumatic artificial muscles: Basic concepts and control issues.* PhD thesis, Vrije Universiteit Brussel, 2005.

[84] Q. Yang, L. Zhang, G. Bao, S. Xu, and J. Ruan. Research on novel flexible pneumatic actuator fpa. In *Proceedings of the 2004 IEEE Conference on Robotics, Automation and Mechatronics, Singapore*, volume 1, pages 385–389, 1-3 December 2004.

[85] S. Diaz Zagal. *Conception et Développement d'un Mini-Actionneur à Muscle Artificiel. Application à la Robotique Médicale.* PhD thesis, Institut National des Sciences Appliquées de Toulouse, 2007.